J. Inst. Eng. India Ser. C
https://doi.org/10.1007/s40032-022-00882-0

ORIGINAL CONTRIBUTION

An Insight into Nylon 6,6 Nanofibers Interleaved E-glass Fiber Reinforced Epoxy Composites

Sachin Chavan[1] · Nand Jee Kanu[2,3] · Sachin Shendokar[4] · Balkrishna Narkhede[5] · Mukesh Kumar Sinha[6] · Eva Gupta[7] · Gyanendra Kumar Singh[8] · Umesh Kumar Vates[9]

Received: 24 December 2021 / Accepted: 12 September 2022

Abstract The research work aims to investigate high-performance nylon 6,6 nanofiber interleaved E-glass fiber reinforced epoxy laminates (prepared using the electrospinning method) which exhibit unique design features in terms of improved mechanical strength. The influences of electrospinning control variables such as the nozzle of spinneret to grounded collector distance, rate of flow, high-voltage power supply, and concentration of polymeric solution to create high-quality nanofibers of specific length and diameter in nanometers are examined. The objectives of the current investigations are to develop delamination-resistant nylon 6,6 nanofibers interleaved E-glass fiber reinforced epoxy structural nanocomposites. The research efforts are thus focused to use electrospinning, vacuum assisted resin transfer molding (VARTM), and glass molding processes to fabricate nanocomposites with electrospun nylon 6,6 nanofibers. The specimens are described and evaluated in accordance with ASTM standards for tensile strength (D 638), flexural or bending strength (D 790-2003) of two-phase composites, and the hand molding or hand layup method are compared to the VARTM process. Two-phase nanocomposites containing nylon 6,6 nanofibers into the polymer matrix (Epolam 5015) are fabricated by glass molding process. The advanced composites are manufactured with primary reinforcement of eight-shaft satin weave pattern glass fiber 7781, with Epolam 5015 matrix and secondary reinforcement of nylon 6, 6 nanofibers with different diameters, i.e., 81, 455, and 1200 nm (multiscale). To achieve the different diameter fibers, statistical tools of design of experiment (DOE), full factorial and Taguchi are employed. Further they are characterized with (1) short beam shear strength (SBS) using ASTM 2344 standard for interlaminar shear strength and (2) double cantilever beam (DCB) using ASTM 5288 standard for Mode I fracture toughness for of three-phase nanocomposites. For better understanding the behavior of nanocomposites, the shear strength between laminate planes, or interlaminar shear strength (ILSS), of nylon 6,6 nanofiber interleaved composites is modeled using the finite element technique.

Keywords Electrospinning · E-glass fibers · Nylon 6,6 nanofibers · Epoxy · Nanocomposites

✉ Sachin Chavan
sschavan@bvucoep.edu.in

1 College of Engineering, Bharati Vidyapeeth Deemed to be University, Pune, India

2 S. V. National Institute of Technology, Surat, India

3 JSPM Narhe Technical Campus, Pune, India

4 Joint School of Nanoscience and Nanoengineering, Greensboro, NC, USA

5 National Institute of Industrial Engineering, Mumbai, India

6 Defence Materials and Stores Research and Development Establishment, Defence Research and Development Organization, Kanpur, India

7 Amity University Uttar Pradesh, Noida, India

8 Adama Science and Technology University, Adama, Ethiopia

9 Amity University Uttar Pradesh, Noida, India

Introduction

Electrospinning is a versatile process for generating ultrathin nanofibers of different materials, and these nanofibers are having potential use in various engineering fields including defense, aerospace, and sports applications [1–4]. Electrospinning is the most preferred process among available processes and considered as a favorable option to prepare ultrathin nanofibers of uniform diameters ranging from 10

Published online: 01 November 2022

to 100 nm, commonly using polymer solutions. Electrospinning has gained much attention in recent research work as it is relatively easy, cost-effective, and applicable in synthesizing ultrathin nanofibers with its simple step-up.

Nylon 6,6 is an engineering thermoplastic and due to its hydrophilic nature, it has been used as water wetting porous membranes in air filtration applications. In addition, nylon 6,6 nanofibers comprising cyclodextrins (CD) are capable to filter organic vapor waste from the surroundings [5-8]. Previous research work suggests that using small quantities (less than 5 wt%) of nylon 6,6 nanofibers (diameter less than 200 nm) as a reinforcing material in composites can provide an uniform dispersion of fibers and a solid interface, resulting in substantial improvements in mechanical behavior due to H-bonding interactions between the reinforcing fibers and the thermoplastic polyurethane (TPU) matrix [7]. Researchers have also studied the effects of electrospinning control variables on the diameter of nanofibers using various tools such as design of experiments (full factorial) and Taguchi [6–10]. According to previous research, an ideal thin film composite (TFC) membrane for engineered osmosis (EO) should feature an ultrathin selective layer with outstanding permselectivity, which is supported by a hydrophilic, highly porous, non-tortuous, and thin support structure. Electrospun nanofibers, a newly developed TFC supporting material, were utilized to create a TFC-EO membrane in which the support structure and selective layer characteristics were independently tuned [11]. Because of its inherent hydrophilicity and superior strength compared to other nanofibers, nylon 6,6 nanofibers produced through electrospinning were employed for the first time to construct the support structure [11]. They recommended covering a hydrophilic nylon 6,6 nanofiber membrane with hydrophilic nylon 6,6 nanofibers to improve deicing [12]. The nylon 6,6 nanofiber membrane's much improved deicing performance shows its potential for practical uses [12]. The polyamide 46 (PA46) PA46's higher hydrophilicity and lower crystal stability compared to PA69; absorbed water droplets produced the plasticizing effect by lowering the percentage of stable crystals, resulting in more stretching of the PA46 polymer jet than the PA69 polymer jet. Depending on the nature of the components in a solution, humidity can impact the surface as well as the inner regions of nanofibers through a variety of events [13]. Due to the flow of charges from polymer solution to ambient humidity in both the Taylor cone and the jet areas, it can cause phase separation, precipitation, and surface charge imbalance. Due to the intrinsic hydrophobicity of the pure drug, the addition of PHMB to the PA6 NFs enhanced the hydrophobicity of the generated scaffolds, as predicted [14]. Hydrophilic surfaces have been shown to provide more appropriate binding sites for cellular adhesion, resulting in more effective scaffold colonization and therefore enhancing the material's cell compatibility [15].

A nanocomposite is considered as a multiphase solid material which incorporates nanosized components into a matrix or at the interface in the form of fibers, particles, or nanotubes. Nanomaterials have high surface-to-volume ratio due to their size effects. In addition to 0.5–3% nanomaterials, the properties of the composites are improved. The choice of the fabrication methods is done on the basis of adjustability of properties and geometry, as well as dimensions, ability and production, tooling expenditure, employee expertise, and further standards. Three-phase composite having one primary reinforcement phase, one matrix phase, and one secondary reinforcement/matrix is called three-phase composite, i.e., primary reinforcement such as E-glass fibers and matrix such as epoxy as well as secondary reinforcement such as nylon 6,6 nanofibers are made with manual layup and VARTM. On the other hand, two-phase composite having one reinforcement and one matrix phase is called two-phase composite, i.e., reinforcement such as nylon 6,6 nanofibers and matrix such as epoxy are typically made by glass molding [15, 16]. The matrix and fibers constitute the two different phases of a two-phase composite. In three-phase composite, one more nanomaterial phase is added in matrix or at interface of two-phase composite. The present investigation aims to fabricate the E-glass fiber reinforced epoxy laminates with interleaved electrospun nylon 6, 6 nanofibers with different diameters.

In orthopedics, a periodontal deficiency is a serious problem. The guided bone regeneration (GBR) membrane is one of the most effective techniques for reconstructing alveolar bone and then repairing or regenerating periodontal defects. By combining a solvent casting and an electrospinning method, a new polyamide-6/chitosan@nano-hydroxyapatite/polyamide-6 (PA6/CS@n-HA/PA6) bilayered tissue guided membrane was prepared. A number of experiments were performed on the produced PA6/CS@n-HA/PA6 composites. The findings demonstrate that molecular interaction and chemical bonding strongly bind the n-HA/PA6 and electrospun PA6/CS layers, enhancing the bonding strength between two different layers. The PA6/CS@n-HA/PA6 membranes have a porosity of 36.90% and an adsorption average pore diameter of 22.61 nm, respectively [17]. Nanofibers have a lot of promise when it comes to enhancing the mechanical performance of optically transparent composites without sacrificing transparency. The reinforcing nanofibers must be thinner than the visible light spectrum's low end (400 nm) to achieve this. A self-mixing co-electrospinning approach was used to prepare electrospun meshes of well-blended nylon 6,6 (PA-6) nanofibers and poly(methyl methacrylate) (PMMA) fibers, from which hot-press molded composite films containing PA-6 nanofibers with various diameters (approximately 100–800 nm) and mass fractions (1–7% wt%) were fabricated [18]. They looked at the properties of nylon 6,6 nanofibers that were produced utilizing an

electrospinning process. The study employed an experimental technique with a quantitative approach. The electrospinning process was used to create nylon 6,6 nanofibers. The SEM results demonstrate that all nylon 6,6 nanofibers have the same shape and produce flawless fibers without bead fiber [19]. The nylon 6,6 nanofibers have uses in medicine, air filters, and capacitor electrodes [20]. Using the Taguchi statistical approach, the research attempts to improve the electrospinning process to generate the smallest nylon 6,6 nanofibers possible. In a combination of formic acid (FA) and dichloromethane, nylon 6,6 solutions were produced (DCM). The FA/DCM ratio and the optimal nylon 6,6 concentration (NY percent) were found [21]. The FA/DCM solvent ratio, as well as the concentration of nylon 6,6, has a substantial impact on the shape of electrospun nanofibers. For a 10 wt% nylon 6,6 solution in 80 wt% FA and 20 wt% DCM, the lowest diameter and narrowest diameter distribution of nylon 6,6 nanofibers (166 ± 33 nm) were produced. Tensile strength, modulus of elasticity, and elongation at break increased by 118, 280, and 26%, respectively, above as-cast. Using a differential scanning calorimeter, the glass transition temperature of nylon 6,6 nanofibers was measured (DSC). The most influential parameter, according to the analysis of variance ANOVA, is NY percent [21]. The article emphasizes the effect of nylon 6,6 electrospun nanofibers interleaved in carbon fiber/epoxy laminates [22]. Nylon 6,6 nanofibers are spun directly onto the surface of the carbon fabric, which is then utilized to make the laminates. SEM, TGA, and DSC analyses were used to characterize the nylon 6,6 fibers. The findings revealed a uniform fiber size distribution and high heat stability [22]. Epoxy resin is now a thermoset polymer that is commonly used in industry. Because its nature as a thermoset resin causes brittleness in the material structure, which results in low toughness, it is of primary importance to modify it with thermoplastic polymers. The aim of the research is to investigate the tensile characteristics and morphological characterization of a PA66 nanofiber yarn reinforced epoxy nanocomposite. Increased nanofiber yarn content resulted in a decrease in elastic modulus and an increase in tensile toughness. Scanning electron microscopic pictures verified river pattern, crack branching, and nanofiber yarn pull-out as toughening mechanisms [23].

It is observed that with the decrease in the diameter of nanofibers, the mechanical properties of such nanocomposites are improved to some extent. The effects of the process parameters are studied [10, 24–26]. Researchers have suggested about the characterization and testing of electrospun nanofiber reinforced composites as that should be accomplished as per the ASTM standards for tensile strength (D 638), flexural strength (D 790-2003), short beam shear (SBS) strength (D 2344), and double cantilever beam (DCB) ASTM 5288 [24–26]. In the present investigation, electrospun nylon 6,6 nanofibers are prepared following the optimized setting of a polymeric solution to fabricate nylon 6,6 nanofibers interleaved E-glass/epoxy structural composites. The investigation was conducted using glass fiber 7781 from INTERGLAS Technologies AG, Benzstrabe 14, D-89155 Erbach, with an eight-shaft satin weave pattern. The finite element analysis is applied to study the shear strength between laminate planes (ILSS) of composite.

Electrospinning of Ultrathin Nylon 6,6 Nanofibers

The electrospinning process is used in the present research work to prepare the nylon 6,6 nanofibers, which are further characterized using SEM. The influences of quality input parameters (such as the nozzle of spinneret to grounded collector distance, applied voltage, flow rate, and further concentration) on the diameters of these nanofibers are investigated for ultrathin nanofibers of nylon 6, 6. The electrospinning setup is shown in Fig. 1. The subparts of the electrospinning setup are mainly the spinneret or needle of dispenser, voltage regulator, rotating drum, and syringe pump which are operated as per the optimized setting to prepare the ultrathin nylon 6,6 nanofibers required for the fabrication of nanocomposites.

After suspending any polymeric solution (via 2–20-mL syringe) in a syringe pump, nanofibers are extracted out of that polymeric solution using electrospinning and electrospun over revolving drum collector (covered with aluminum foil) usually needs to be grounded. In previous researches, drum collector is set to rotate in the range between 900 and 1300 rpm [8]. Therefore, ultrathin nanofibers are electrospun on the rotating drum at around 1000 rpm. The effects of control parameters such as the nozzle of spinneret to grounded collector distance, rate of flow, high-voltage power supply, and further concentration of the polymeric solution are studied in detail to find their effects on the diameter of nanofibers. The effects of control parameters are studied during the optimization of electrospun polymer nanofibers.

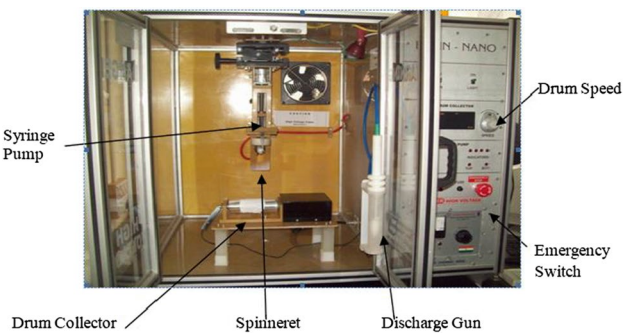

Fig. 1 The electrospinning setup

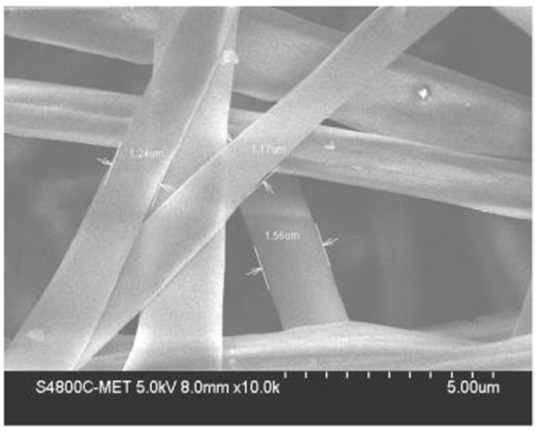

Fig. 2 Sample 5 (1200 nm): 10 cm, 0.2 mL/h, and 20 kV

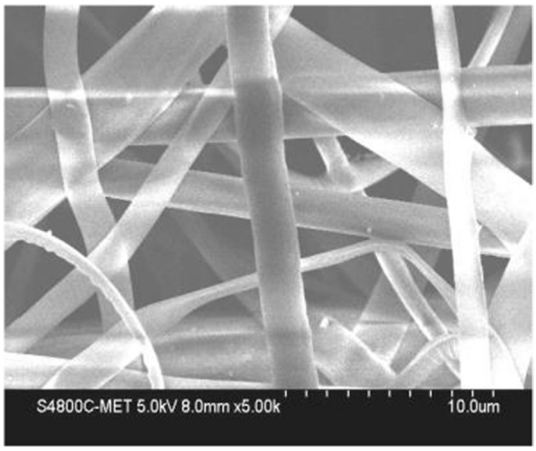

Fig. 3 Sample 6 (1400 nm): 10 cm, 0.3 mL/h, and 20 kV

Results and Discussion

Preparation of Nylon 6,6 Nanofibers

The solutions for electrospun nanofibers are prepared by mixing 18 and 20% nylon 6,6 in 10 mL of 98% methanoic acid (HCOOH, a reagent). The analysis tool such as design of experiment (DOE), namely full factorial, and Taguchi, is utilized to explore the influences of control parameters on the diameter of nanofibers.

Few sample images of nylon 6,6 nanofibers examined under SEM and diameters are assessed in ImageJ software as shown in Figs. 2, 3, 4 and 5. The nanofibers produced are in different diameter range, and distribution is uniform in some cases and apparently fine for other. Moreover, for calculation part average diameter of nanofibers need to be finalized that is the reason for assessment of average diameters of nylon 6,6 nanofibers using their SEM images in ImageJ software.

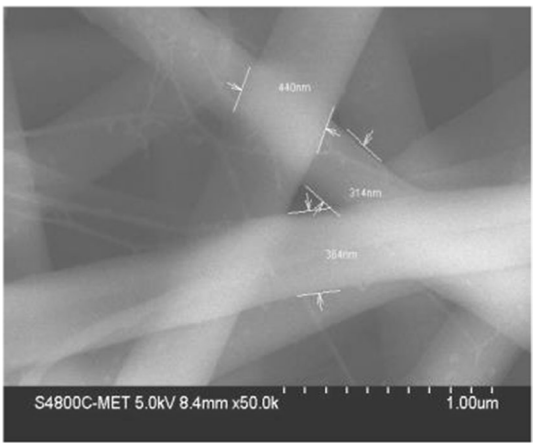

Fig. 4 Sample 3 (360 nm): 15 cm, 0.2 mL/h, and 15 kV

Table 1 Specifications of electrospinning set up

Specifications	Model–VI
Power supply	0–40 kV
Voltage (kV)	1 Ma
Syringe size needle	*Syringe pumps of capacity* 2–20 mL
Flow rate (mL/h)	0.05–100 mL/h
Rotating drum ($l \times dia.$)	125 × 40 (mm)

The 2^k factorial design initially with three parameters, the nozzle of spinneret to grounded collector distance, applied voltage and flow rate, is used to optimize the above input process parameters at two levels such as low and high as listed in Table 1 and 2. With the increase in voltage of 15 kV (at 15 cm distance and 0.2 mL/h flow rate) and using a solution having 18% nylon 6,6 in 10 mL of 98% HCCOH, the diameter of the nanofibers is measured around 360 nm. Two iterations were taken at different intervals and average diameter is considered for further calculation. For each iteration diameter is measured by using average values diameter produced with respective parameter. For example, consider the reading no. 03 where diameter synthesized is 353 nm for first iteration and 367 nm for second iteration. The SEM image for these two readings was studied.

The regression equation for diameter of nylon 6,6 nanofibers is shown using Eq. (1).

$$\text{Diameter (nm)} = 222 - 61.8A - 29.3B + 13.2C \quad (1)$$

After using three parameter at two levels, the target of diameter below 100 nm is not achieved.

So further, L_9 orthogonal array (Taguchi) is selected for parametric study to optimize the diameter (Table 3). Here,

four parameters and three levels are used. The electrospun nanofibers are prepared following the optimized setting of the solution of nylon 6,6 in methanoic acid such as the nozzle to spinneret to grounded collector distance (10, 15 and 20 cm), rate of flow (0.2, 0.5 and 1 mL/h), high-voltage power supply (15, 20 and 25 kV), and concentration (18, 20 and 25% nylon 6,6 nanofibers in 10 mL of 98% HCCOH) (Fig. 5).

Table 2 Experimental results for full factorial DOE

Sr. no.	Distance(cm) *A*	Voltage (kV) *B*	Flow rate (mL/h) *C*	Iteration no. 01 diameter (nm)	Iteration no. 02 diameter (nm)	Average diameter (nm)
1	15	20	0.2	505	515	510 ± 35
2	15	20	0.3	610	588	600 ± 42
3	15	15	0.2	353	367	360 ± 75
4	15	15	0.3	423	438	430 ± 45
5	10	20	0.2	1197	1207	1200 ± 14
6	10	20	0.3	1413	1396	1400 ± 70
7	10	15	0.2	883	915	900 ± 07
8	10	15	0.3	1024	982	1000 ± 51

Table 3 Experimental reading for L_9 orthogonal array

Sr. no	Distance (cm) *A*	Flow rate (mL/h) *B*	Voltage (kV) *C*	Concentration (%) *D*	Iteration no. 01 diameter nm	Iteration no. 02 diameter nm	Average diameter nm
1	10	0.2	15	18	982	1016	999 ± 53
2	10	0.5	20	20	689	718	703 ± 41
3	10	1	25	25	1185	1217	1201 ± 29
4	15	0.2	20	25	574	0612	593 ± 32
5	15	0.5	25	18	444	447	445 ± 36
6	15	1	15	20	610	641	625 ± 48
7	20	0.2	25	20	79	84	81 ± 80
8	20	0.5	15	25	110	125	117 ± 52
9	20	1	20	18	90	94	92 ± 21

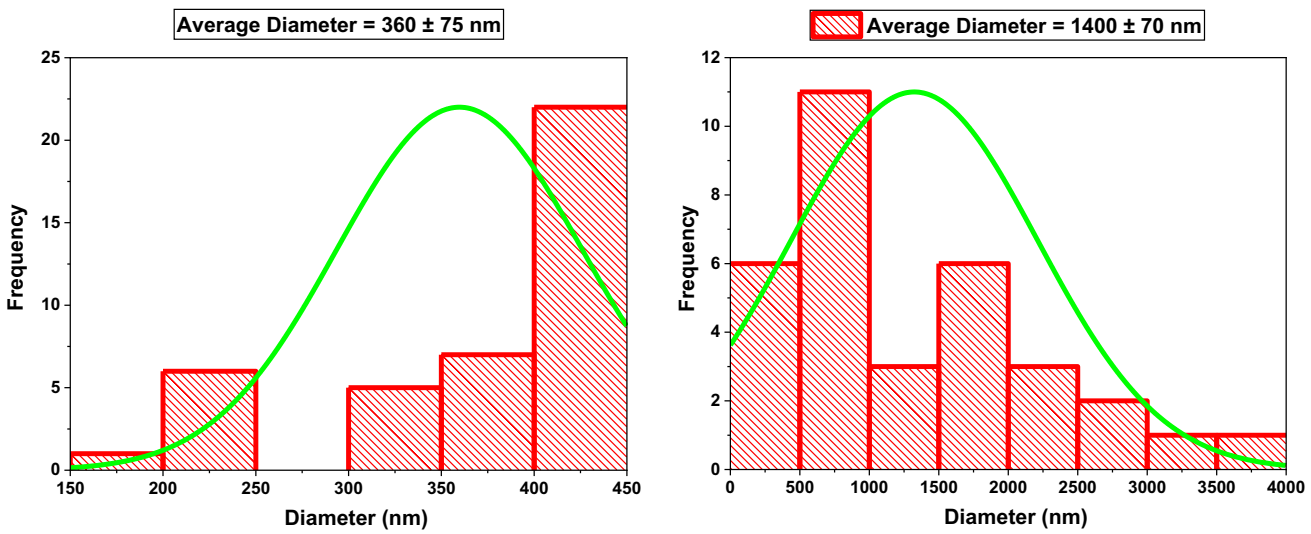

Fig. 5 Diameter distribution for samples 3 and 6

The *F-value* (*F-ratio* based on *F-distribution* values) at the 95% level of confidence is around 7.71, and thus, conclusions are drawn about the diameters that they would depend significantly on the factors such as the nozzle to spinneret to grounded collector distance (cm), rate of flow (mL/h), and high-voltage power supply (kV). The analysis of variance (ANOVA) is used to explore the importance of distance (*A*) (around 82.47%) on the diameter of nylon 6,6 nanofibers (as shown in Figs. 6, 7, 8, and 9), where the variables such as *A, B, C,* and *D* are used to express the nozzle of the spinneret to grounded collector distance (cm), the rate of flow (mL/h), the voltage supply (kV), and concentration (%). The experimental diameters of nylon 6,6 nanofibers are plotted against the theoretical diameters (Fig. 10) and found to be in close agreement with each other.

Taguchi analysis (while considering L_9 orthogonal array of four levels and three parameters) confirmed that the distance had a significant influence around 88.65%, and the influences of the remaining factors such as *B*, *C*, and *D* are not so significant, i.e., they are around 5.62, 2.07, and 2.5%, respectively. With the increase in distance, the diameter is reduced as the span available for elongation is more (Fig. 11). With the increase in flow rate from 0.2 to 0.5 mL/h, the diameter is reduced to some extent because of other process parameters at the corresponding level of interaction. With further increase in the flow rate, the time required for elongation is reduced and that had resulted in an increase in diameter (Fig. 11). The resultant variation is not so significant, and thus, the effect of flow rate is considered less. With the increase in voltage from 15 to 20 kV, the diameter is reduced. Furthermore, with an increase in the voltage from 20 to 25 kV, the diameters of electrospun nanofibers are increased to some extent as demonstrated in Fig. 11. The possible combination is not so significant, and thus, the effect of voltage is considered less. It is observed that with the increase in concentration from 18 to 20%, the diameters of electrospun nanofibers are increased.

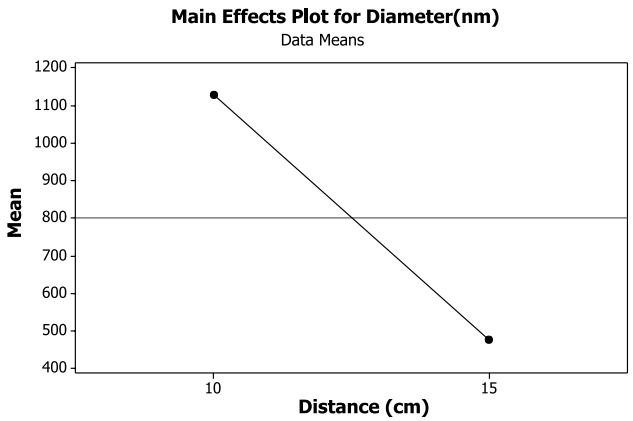

Fig. 6 Distance versus diameter

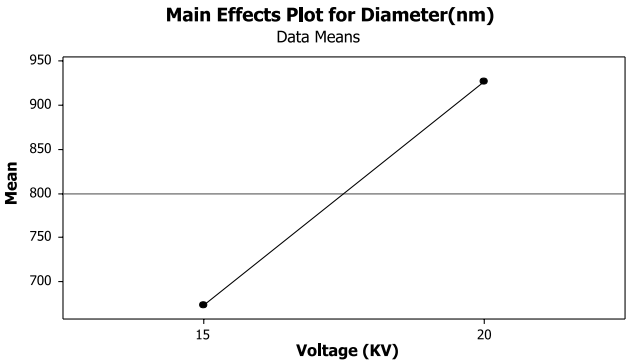

Fig. 7 Voltage versus diameter

However, with a further increase in the concentration from 20 to 25%, the diameters of electrospun nanofibers are reduced as illustrated in Fig. 11. The possible combination is not so significant and thus the effect of concentration is considered less. In Fig. 12, the interactions between the rate of flow, voltage, and concentration are shown and the effects of the contributions of those interactions are found to be negligible.

The regression analysis equation for electrospun nanofibers is shown using Eq. (2).

$$\text{Diameter (nm)} = 1209 - 436A + 40.8B - 1.7C + 61.8D \tag{2}$$

Regression Eq. (1) is for full factorial DOE based on analysis of variance. Furthermore, three input parameters such as the nozzle of spinneret to grounded collector distance, applied voltage, and flow rate were examined at two levels such as low and high to optimize the settings for minimum average diameter of nanofibers. On the other hand, Eq. (2) is derived for Taguchi L9 orthogonal array. Four input process parameters such as the nozzle of spinneret to grounded collector distance, applied voltage, flow rate, and concentration and three levels were examined for the optimized settings.

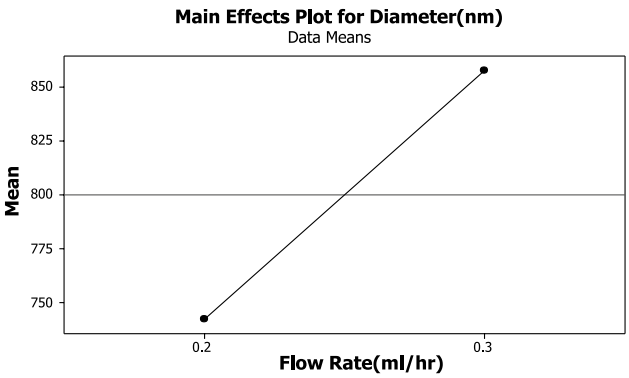

Fig. 8 Flow rate versus diameter

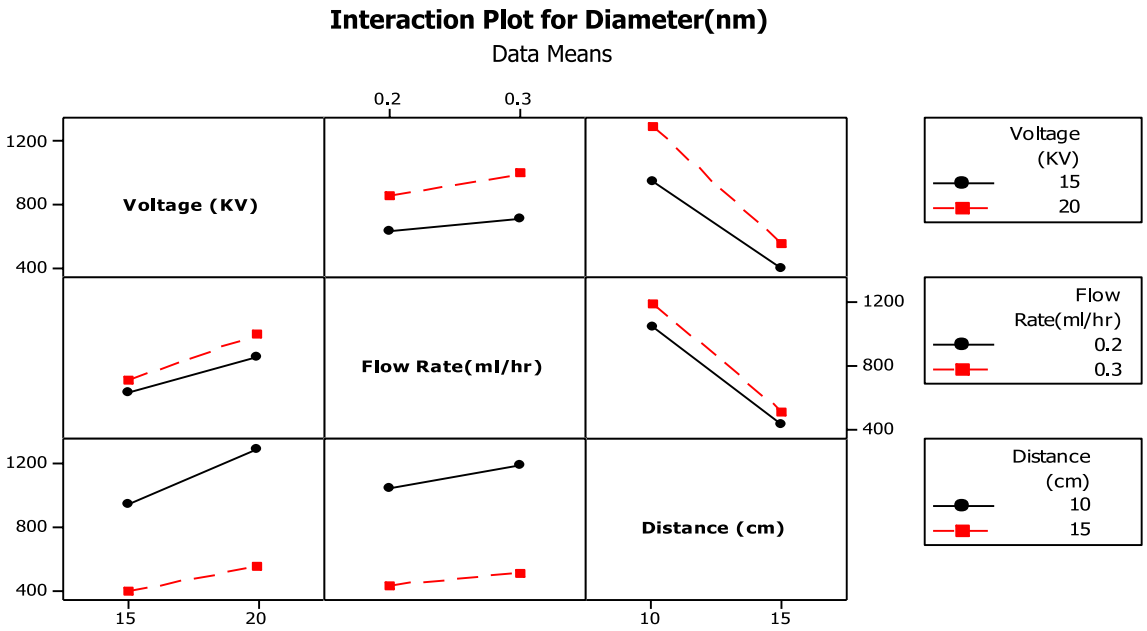

Fig. 9 Interaction plot of DOE-full factorial for nylon 6,6 nanofibers

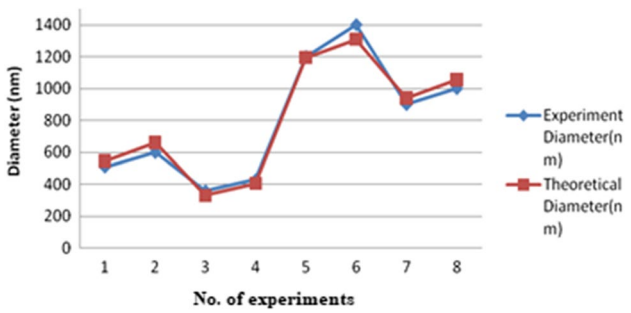

Fig. 10 DOE-Experimental diameters versus theoretical diameters of electrospun nylon 6,6 nanofibers

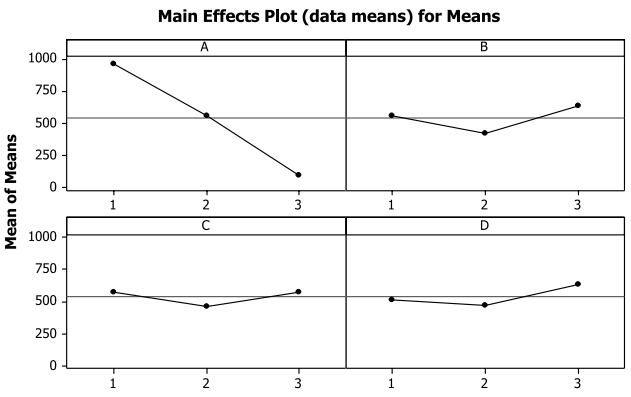

Fig. 11 Taguchi-Effects of process parameters on diameters of nanofibers

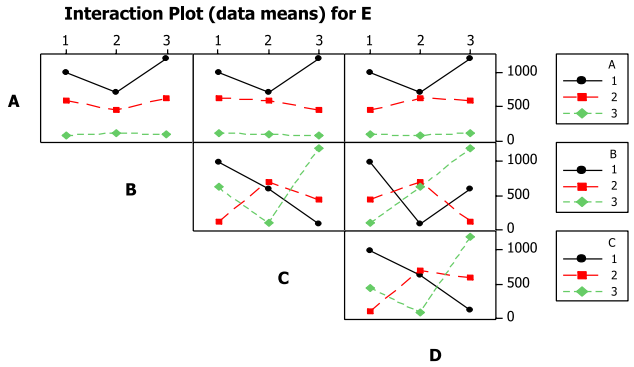

Fig. 12 Taguchi-Interaction plot for electrospun nylon 6,6 nanofibers

As concentration was not taken for full factorial DOE, hence there is no relation of parameter D of Eq. (2) with Eq. (1). These experiments were done to optimize the diameter of nylon 6,6 nanofibers. The graphs in Fig. 13 show exactly the reverse impacts of process variables on the diameters of electrospun nanofibers in comparison with the main effects that is correct for the condition "the less we have, the better." The experimental diameter values are found to be in agreement with the theoretical diameter values (Fig. 14).

The experiments were conducted using a 2^k factorial design, with independent variables (distance between the spinneret and collector, flow rate, voltage for full factorial DOE, and low, medium, and high for L_9 orthogonal array—Taguchi, respectively) being the distance between the spinneret and collector, flow rate, voltage for full factorial DOE,

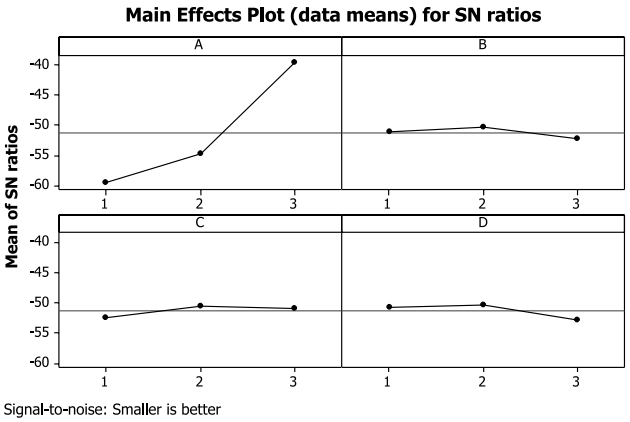

Fig. 13 Process parameters versus diameters of nanofibers

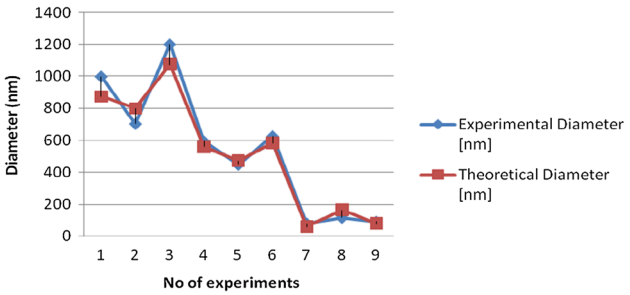

Fig. 14 Taguchi-Experimental diameters versus theoretical diameters of nylon 6,6 nanofibers

and additionally concentration was considered in case of L_9 Orthogonal Array—Taguchi. As a result, full factorial DOE had eight observations, whereas L9 orthogonal array—Taguchi—had nine. The diameters of all samples were measured using scanning electron microscopy (SEM). A few pictures of nylon 6,6 nanofibers studied under a scanning electron microscope. All procedure parameters were used to make the ultrathin nanofibers.

It was done to determine the importance of the contributions of the different parameters in obtaining the nanofibers' lowest diameter. The correction factor, CF, was calculated (to compute the sum of squares of input variables). Following that, the sum of squares values for various interactions were evaluated. The error ratio was calculated when the errors were pooled together. Furthermore, using the *F*-distribution table to calculate the *F* ratio, the authors discovered that the *F* value for 95% level of confidence is 7.71, and it was concluded that the diameters of nanofibers are dependent on several parameters. Because each input variable has two levels in full factorial DOE and three levels in Taguchi and has one degree of freedom, the minimum diameter of nanofibers was calculated using an ordinary regression model after substituting acceptable values for the interaction effects. Equations (1) and (2) demonstrate the general form of the regression analysis Eq. (2). Only the border regions are covered by the models. MINITAB 17 software was used to plot the major effects and interactions plots for the means of the average diameters (nm) with regard to the important process parameters.

The objective of the present investigation is fulfilled after synthesis of 81 nm diameter of nylon 6,6 nanofibers following the optimized setting of a polymeric solution having 20% nylon 6,6 in 10 mL of 98% HCCOH while maintaining voltage at 25 kV, distance at 20 cm, rate of flow at 0.2 mL/h and speed of drum collector around 1000 rpm. These ultrathin bead-free nanofibers are having a large surface area and thus are suitable for the fabrication of nylon 6,6 nanofibers interleaved E-glass fiber reinforced epoxy laminates to fulfill the objective of the present research. In Fig. 15, a recent development is shown for the preparation of ultrathin electrospun nylon 6,6 nanofibers, and 81 nm diameters are found to be the lowest in their range so far [27–32].

Manufacturing of Nylon 6,6 Nanofibers Interleaved E-glass Fiber Reinforced Epoxy Laminates

The investigation was conducted using glass fiber 7781 with an eight-shaft satin weave pattern from INTERGLAS Technologies AG, Benzstrabe 14, D-89155 Erbach. Hand layup is a popular and cost-effective manufacturing method for fabricating two-phase and three-phase nanocomposites. This technique is used to create large-scale composite constructions. To cover the mold, a layer of LOCTITE® FREKOTE FrewaX (a semi-permanent releasing agent) is applied first (Fig. 16). Alternatively, the plastic bag may be used for the same purpose. Using rollers, excess resins are removed from the setup; however, unevenness in the thickness became the limitation of the method. Also, the authors observed large amounts of voids which is entrapped into the composites using the method, thereby the quality and mechanical performance is deteriorated. VARTM, on the other hand, is used to fabricate composites (uniform thickness and less porosity) with improved mechanical properties.

The vacuum-assisted resin transfer molding (VARTM) process is preferred in the present investigations due to due to good fiber weight fraction as compared to hand molding process and less tooling cost and further the method is environmental friendly as compared to resin transfer molding process. The vacuum bag had replaced the metal mold in the VARTM technique (Figs. 17 and 18). The flat-faced square panels are commonly employed in research projects, and their sizes are determined by the specimens to be manufactured. The flat-faced square panel's most common size is 30 by 30 cm. Several lamina (glass fiber 7781) are piled up to create the whole laminated structure based on the thickness requirements of the specimens. High-density

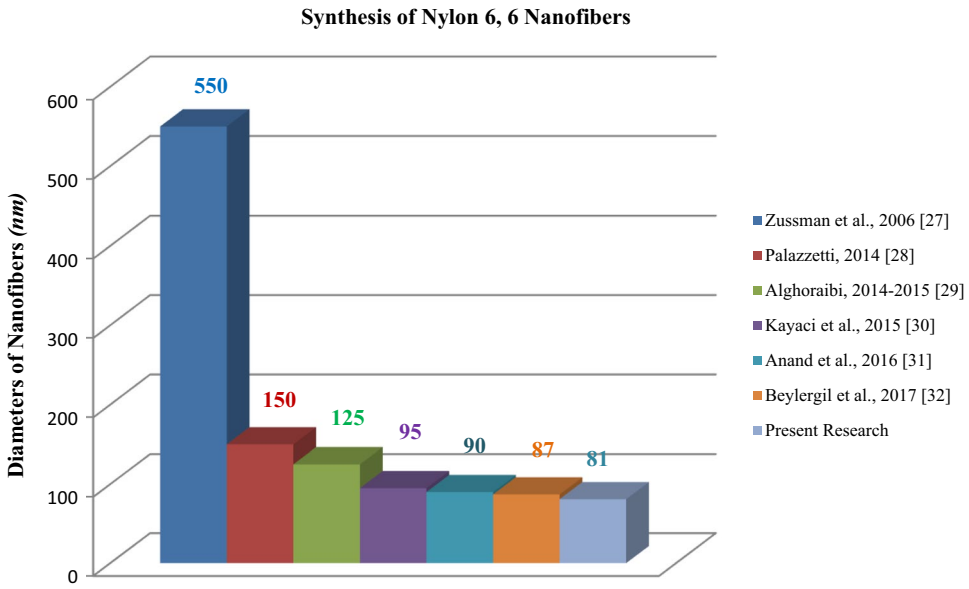

Fig. 15 Diameters (nm) of nylon 6, 6 nanofibers

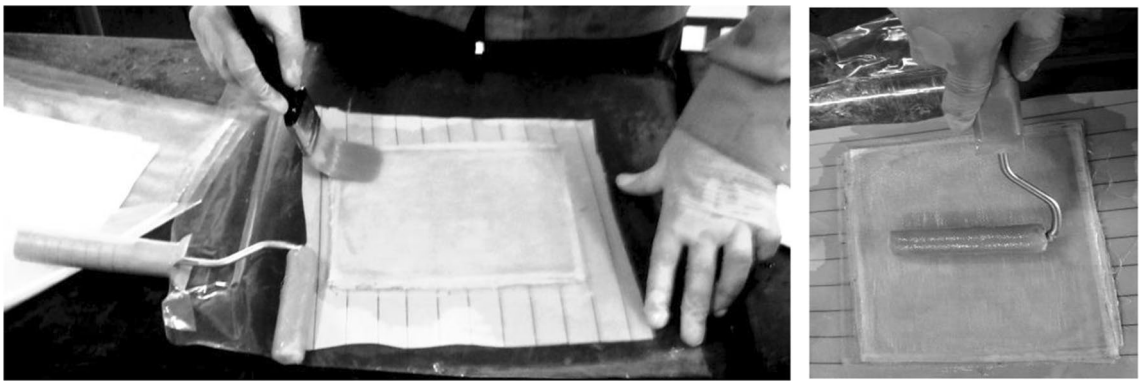

Fig. 16 Hand molding process

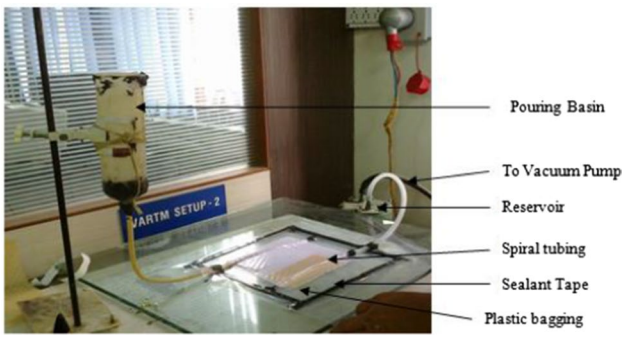

Fig. 17 Actual VARTM setup

polyethylene tubes make up the supply and suction channels (HDPE). Spiral-cut tubing is used as a supply and suction route for resin impregnation. The tube is generally placed on the top or bottom of the perforated Teflon fabric or resin flow media, near to the fabric layup at the resin supply end.

To collect resin from the top and bottom of the perforated Teflon cloth, a tube is constructed near the setup (resin flow media). The tube is built about *2 inches* away from the laminate manufacturing setup near the suction point, which is directly opposite to the supply point. The resin circular tubing is connected to the storage (delivery side) by tubing connectors made of polytetrafluoroethylene (PTFE), and the vacuum pump is connected to the suction end by tubing connectors made of polytetrafluoroethylene (PTFE). In the configuration, the two ends, such as the supply and suction ends, are assembled diagonally opposite one other. The polysulfide sealant tape is used to secure the edges of the stacked plies. The vacuum bag is composed of temperature-resistant Teflon sheet with a thickness of *25 microns*. The vacuumed container (under *1 bar* vacuum pressure) is fixed over the sealant and the setup is

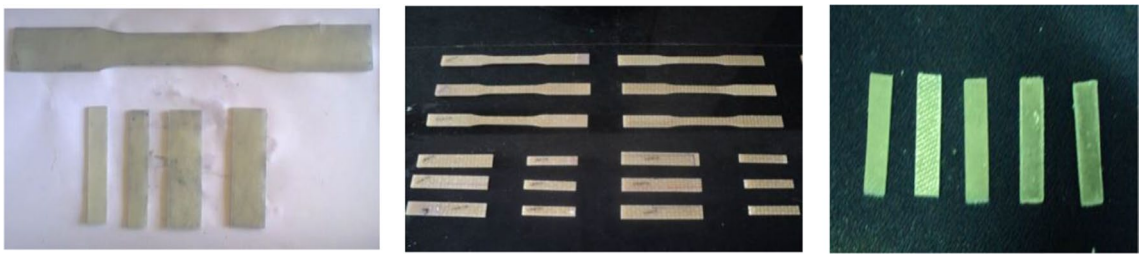

Fig. 18 Specimen cut as per ASTM Standard

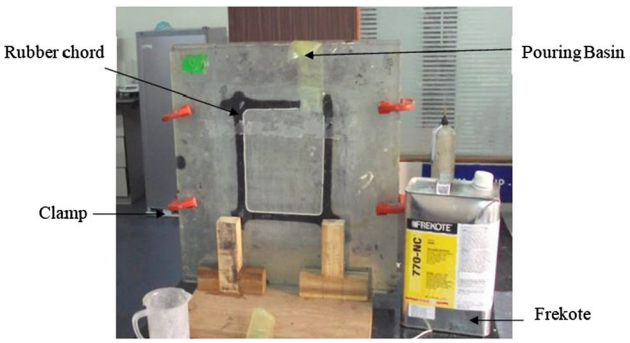

Fig. 19 Glass mold setup

monitored for any leakage in the next few minutes (about 1 h). The clamps, quite adjustable, are utilized in the suction line (at PTFE tubing) and monitored for any possible leakage. Once it is confirmed that there is no leakage, then the vacuum pump is turned off. In the present research, the matrix solution is developed using Epolam 5015 and curing agent, mixed in the ratio of 100:30. The resin solution is allowed to wet the E-glass fibers by adjusting the clamps while the suction line is closed during the overnight impregnation activity and then left for curing at normal temperature. Once the vacuum bag is free of leaks and the resin is ready, resin impregnation of the fabric layup is accomplished by pouring resin into the resin reservoir and slightly opening the adjustable clamp to allow the resin to flow through. During resin impregnation, the adjustable clamp on the suction end is kept closed at all times. The curing cycle for the Epolam 5015 is 24 h at room temperature, according to supplier Axon India's suggestion. The glass fabric 7781 laminates were mixed with resin initially to guide them (resin) through gaps between the strands.

Glass Molding: as shown in Fig. 19, the glass molding method is the easiest way to make a two-phase polymer nanocomposite with nanocomponent. Two borosilicate flat square glass plates are included. As a releasing agent, Henkel's "Frekote 55-NC" is applied to the borosilicate glass. The size and form of plagues are determined by the rubber chord's dimensions. The sizes and forms of the specimens (plagues) in the example are inspired by the shapes of rubber strands. A 2-mm elastic wire is often used to construct a 2-mm sample. Umeco sealant has been chosen for the work because the mold is mainly sealed with polysulfide sealer. The resin solution (Epolam 5015) is poured into a Teflon gate through opening. The glass mold is held in place with four hand clamps to guarantee equal thickness of the specimens and then permitted to cure at room temperature overnight.

Testing on Two-Phase and Three-Phase Nanocomposites

The E-glass (fiber 7781)/epoxy (Epolam 5015) structural nanocomposites with interleaved nylon 6,6 nanofibers are fabricated for the present investigation to overcome delamination problems. The concept of electrospun nylon 6,6 nanofibers at interfacial regions between E-glass fibers and matrix is developed to improve the fracture toughness. A few efficient manufacturing processes is evaluated in the present investigation based on their easiness to produce cost-effective and outstanding composite structures. The two-phase nanocomposites manufactured by glass molding (different diameters of nylon 6,6 nanofibers and Epolam 5015 as matrix) is tested for their mechanical properties. Various samples of two-phase and three-phase nanocomposites are fabricated and then tested for their tensile, flexural, and short beam shear (SBS) strength and double cantilever beam (DSB) as per ASTM standards to study their shear strength between laminate planes (ILSS).

The two-phase composite prepared by hand mold had some voids in the fabricated structures and that became the limitation of manufacturing processes as these air bubbles are responsible for micro cracks at the initial stages of failure of structures. To avoid the voids and increase the strength of composite VARTM is used for which fiber weight fraction plays crucial role to the same. The details about fiber weight fractions of E-glass fibers for a few manufacturing processes such as hand molding and VARTM are illustrated in Table 4. In general, with the increase in fiber weight fraction, the strength of the composites is improved. The expression of the volume of fiber is shown using Eq. (3). There are several causes for void formation such as mechanical air entrapment

Table 4 Fiber weight fraction estimation for VARTM and hand molding process samples

VARTM	Hand molding
a = One hundred and seventy	a = Two hundred
b = Sixty	b = Seventy
w = One hundred and twenty	w = One hundred and twenty
$\rho_m = 1.150$	$\rho_m = 1.150$
$\rho_f = 1.80$	$\rho_f = 1.80$
$V_f = 63\%$	$V_f = 54\%$

during resin flow (main cause), gas created due to chemical reactions during cure, and nucleation of dissolved gases in the resin. In two phases, voids are created due to process constraint of rubber chord, leakage, and chemical reaction during curing. Due to this limitation more voids generated in the two-phase (reinforcement material: nylon 6,6 nanofibers; matrix: epoxy) composites. In three phases (reinforcement material: nylon 6,6 nanofibers and glass fibers; matrix: epoxy), as mentioned air entrapment during resin flow or processing method, i.e., hand mold where the void are formed due to in proper rolling, entrapped gases and excesses resin, whereas VARTM used vacuum pump to vacuumed the mold which avoid the formation of void. Nanofibers reacted at interphase and acquired the space in between fiber and matrix and further, reduced voids in nanocomposites. Volume fraction of fibers is kept as per ASTM D2584 and as per Muffle furnace burn-out. The fiber volume fraction calculated in manuscript is done for the sample without nanofibers. For instance, the weight of neat composite panel prepared using VARTM for size around 200 mm by 157 mm is 132 g, and thus, 1.32 g nylon 6,6 nanofibers (around 1%) are reinforced in the respective nanocomposite panel [sheets of nylon 6,6 nanofibrous mats placed at the interfaces—20 GSM (g/m^2)]. In polymer composites, the fiber is the principal load-bearing element. When a result, as the fiber volume fraction (i.e. percentage) increases, so does the strength. Because of the good fiber volume fraction in the Hand Molding process, the same effect was found in the VARTM process. Further vacuum is utilized to infuse the resin, which originally vacuumed the performance and resulted in less air bubble traps or voids. As the number of voids decreases, the likelihood of failure decreases, improving the material's properties.

$$V_f = \frac{\rho_c - \rho_m}{\rho_f - \rho_m} \tag{3}$$

where ρ_c = density of composite, ρ_m = density of matrix, ρ_f = density of fiber, a = sample weight in the air, b = the apparent weight of a sample fully submerged in water, w = the weight of a partly submerged wire in water, 0.9995 = water's density.

The density of composite,

$$\rho_c = \frac{a}{(a + w - b)}$$

The characterization results and evaluation of VARTM with hand layup for tensile (ASTM D 638) and flexural strength (D 790) four different material systems are studied which are listed in Tables 5, 6, 7, 8, 9, 10, 11, 12, and 13. The evaluation is done as per ASTM standards as shown in Figs. 20 and 21.

Table 5 Tensile Strength of Glass fiber Epoxy Epon 862 composite

Tensile strength (ASTM D638) (MPa)		
Iterations	VARTM	HAND MOLD
1	364.40	301.44
2	421.42	316.00
3	366.14	305.71
4	400.12	310.34
5	367.85	305.09
Mean	383.99	307.71

Table 6 Flexural strength glass fiber epoxy Epon 862 composite

Flexural strength ASTM D 790-2003 (MPa)		
Iterations	VARTM	HAND MOLD
1	76.45	40.58
2	68.83	55.56
3	74.84	43.63
4	78.98	50.87
5	67.79	42.31
Mean	73.38	46.59

Table 7 Tensile strength: triaxial glass fiber unsaturated polyester resin (roof lite) composite

Tensile strength (ASTM D638) (MPa)		
Iterations	VARTM	HAND MOLD
1	435.37	358.34
2	429.76	341.46
3	437.87	363.15
4	421.34	351.54
5	447.00	377.51
Average	434.27 MPa	358.4 MPa

Table 8 Flexural strength: triaxial glass fiber unsaturated polyester resin (roof lite) composite

Flexural strength ASTM D 790-2003 (MPa)		
Iterations	VARTM	HAND MOLD
1	153.76	120.82
2	150.86	117.98
3	160.76	128.65
4	148.98	120
5	155.64	117.55
Average	154 MPa	121 MPa

Table 9 Tensile strength: biaxial glass fiber vinlyester resin composite

Tensile strength (ASTM D638) (MPa)		
Iterations	VARTM	HAND MOLD
1	270.14	220.57
2	275.51	222.38
3	269.76	225.79
4	279.90	226.33
5	272.20	219.46
Average	273.50 MPa	222.90 MPa

Table 10 Flexural strength: biaxial glass fiber vinlyester resin composite

Flexural strength ASTM D 790-2003 (MPa)		
Iterations	VARTM	HAND MOLD
1	40.12	128.34
2	43.24	125.81
3	38.71	131.27
4	39.92	124.56
5	48.00	135.00
Average	42 MPa	129 MPa

Due to less thickness the sample does not break, and hence maximum value is reported

Table 11 Tensile strength: Glass Fiber 7781 Epoxy Epolam 5015 composite

Tensile strength (ASTM D638) (MPa)		
Iterations	VARTM	HAND MOLD
1	520	410
2	515	405
3	529	412
4	520	420
5	515	387
Average	520 MPa	407 MPa

Table 12 Flexural Strength: Glass Fiber 7781 Epoxy Epolam 5015 composite

Flexural strength ASTM D 790-2003 (MPa)		
Iterations	VARTM	HAND MOLD
1	214.14	123.56
2	220.16	130.51
3	217.91	129.04
4	215.45	127.82
5	222.06	124.07
Average	218 MPa	127MPA

Glass fiber and epoxy are the first two materials in the material system I (Epon 862 and Epicure as hardener)

Material system II: Triaxial Glass fiber with Unsaturated Polyester Resin (Roof lite)

Material system III: Reinforcement = Biaxial Glass fiber and Matrix-Vinlyester Resin

Material system IV: Glass Fiber 7781/Epolam 5015

The universal testing machine (UTM) is used to conduct the three point bend tests on the specimens which is manufactured using glass molding as per ASTM D 790 standard to test the bending strength of the laminates. A rectangular specimen, supported on two roller supports, is loaded through a loading nose at the center of the laminate. A support of span-to-depth ratio is 16:1. The specimen is deflected until rupture took place at the upper surface of the specimen or until a maximum strain of 5% is reached. Theplagues are prepared as per ASTM D 790-2003. The evaluation results of the standard specimen are shown in Fig. 22.

Three-phase nylon 6,6 nanofibers interleaved E-glass/epoxy (Epolam 5015) structural composite (5% weight of nylon 6,6 nanofibers having diameter 1200 nm) is evaluated. The authors have observed deterioration in flexural properties (as shown in Table 13) because of the voids in the glass molding process. At first, the glass mold is heated to overcome the limitation as much as possible, but later on the mold is replaced with an aluminum plate to restrict the formation of voids. But the substantial strength is not increased. So further FEM model is done to study effect of nanofibers in two-phase composite.

Short beam shear (SBS) strength (ASTM D 2344) characteristics is the objective of the present investigation (Tables 14, 15, 16, 17, and 18). At first, the evaluation details of short beam shear (SBS) strength tests are discussed along with geometry of the specimen (Fig. 23) and mechanical properties of the three-phase nanocomposites as per ASTM D 2344. A flat-faced laminate (ten layers of E-glass fibers) of three-phase nanocomposites [length of the specimen, l (six times the thickness); breadth of the specimen, b (two times the thickness); and span of the specimen, s (four times the thickness)], is studied for its short beam shear (SBS) strength using universal testing machine (UTM) (Fig. 23).

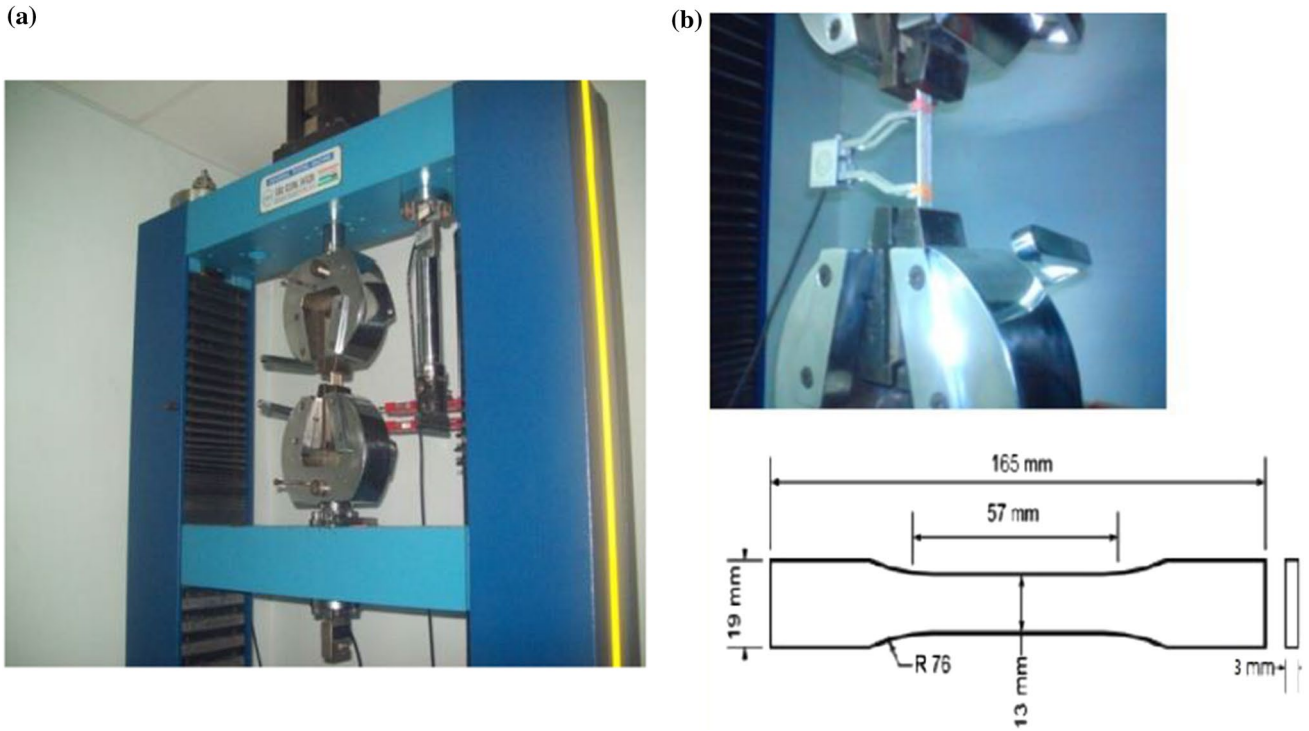

Fig. 20 Tensile test setup. **a** Overall view. **b** Specimen view

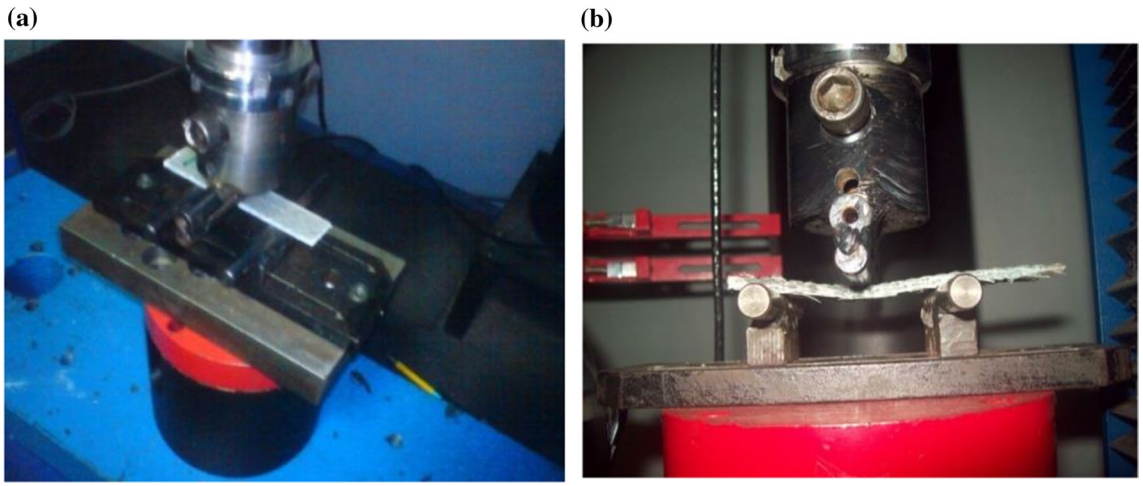

Fig. 21 Three point flexural test setup. **a** Top view. **b** Front view

The frequency of evaluating the results (rate of testing in terms of crosshead progress of 1 mm/min as per ASTM D 2344 standard) is one of the critical aspects to realize considering the time needed (a) to process the output using the setup and (b) to observe the reaction of specimens against applied loads. The limiting cross-head movement is evaluated against the failure assumption. The specimens are failed when there is a load drop of 50%, or when divided into two different halves, otherwise the crosshead travel is supposed to exceed the normal thickness of specimens. The three-phase composites had a 50% load drop criterion for failure or for terminating the test. The plots are created between (a) load and crosshead displacement, and (b) maximum load and load until failure. The short beam shear strength is shown using Eq. (4).

Table 13 Flexural strength comparisons for neat and nylon 6, 6 nanofibers with diameter 1.2 µm manufactured with the help of glass molding process

Flexural strength ASTM D 790-2003 (MPa)		
Iterations	Neat	With nylon 6, 6 nanofibers
1	93.56	87.98
2	100.67	89.23
3	97.56	85.36
4	88.45	89.98
5	84.11	89.10
	92.87	88.33

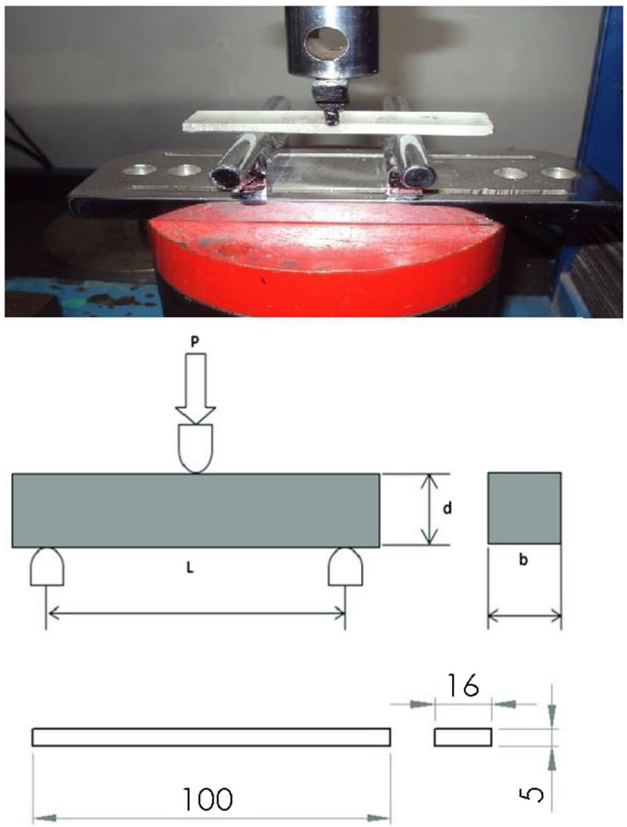

Fig. 22 Test setup for flexural strength and specimen

$$F_{\text{sbs}} = 0.75\left(\frac{P_{\text{m}}}{bh}\right) \tag{4}$$

In Eq. (4), F_{sbs}, P_{m} b, and h are short beam shear (SBS) strength (MPa), width, and thickness of specimen in mm, respectively.

HSBSNeat: Neat Hand mold coupons without nylon 6,6 nanofibers

Table 14 SBS: results for hand molding

Sr. no	Iterations	SBS (MPa)	Avg. SBS (MPa)	SD
1	HSBSNeat 1	21.25	21.08	0.2529
2	HSBSNeat 2	21.13		
3	HSBSNeat 3	20.64		
4	HSBSNeat 4	21.38		
5	HSBSNeat 5	21.01		
6	HSBSNano 1 (1%)	25.97	26.06	0.0928
7	HSBSNano 2 (1%)	26.18		
8	HSBSNano 3 (1%)	26.04		
9	HSBSNano 4 (1%)	25.95		
10	HSBSNano 5 (1%)	26.15		

Table 15 SBS: results for VARTM with interleaved 1200-nm-diameter nylon 6,6 nanofiber

Sr. no	Iterations	SBS (MPa)	Avg. SBS (MPa)	SD
1	VSBSNeat 1	24.43	24.64	0.01
2	VSBSNeat 2	24.53		
3	VSBSNeat 3	24.59		
4	VSBSNeat 4	24.65		
5	VSBSNeat 5	24.97		
6	VSBSNano 1 (1%)	20.71	19.04	0.005
7	VSBSNano 2 (1%)	19.32		
8	VSBSNano 3 (1%)	19.33		
9	VSBSNano 4 (1%)	18.98		
10	VSBSNano 5 (1%)	16.84		
11	VModifySBS Nano 1 (1%)	30.28	30.77	0.015
12	VModifySBSNano 2(1%)	30.95		
13	VModifySBSNano 3 (1%)	30.81		
14	VModifySBSNano 4 (1%)	30.96		
15	VModifySBSNano 5 (1%)	30.89		

Table 16 SBS: results for VARTM with interleaved 455 nm diameter nylon 6,6 nanofibers

Sr. no	Iterations	SBS (MPa)	Avg. SBS (MPa)	SD
1	VModifySBSNano 1 (1%)	32.12	32.19	0.06
2	VModifySBSNano 2 (1%)	32.49		
3	VModifySBSNano 3 (1%)	31.56		
4	VModifySBSNano 4 (1%)	32.44		
5	VModifySBSNano 5 (1%)	32.35		

Table 17 SBS: results for VARTM with interleaved 81 nm diameter nylon 6,6 nanofibers

Sr. no	Iterations	SBS (MPa)	Avg. SBS (MPa)	SD
1	VModifySBSNano 1 (1%)	36.28	36.39	0.06
2	VModifySBSNano 2 (1%)	36.51		
3	VModifySBSNano 3 (1%)	36.88		
4	VModifySBSNano 4 (1%)	36.30		
5	VModifySBSNano 5 (1%)	36.02		

Table 18 Comparison of Values of SBS for Neat and secondary reinforcement of nylon 6,6 nanofiber diameter 81, 455 and 1200 nm

Sr. no	Iterations	(MPa)	Percentage enhancement (%)
1	Neat-SBS	24.64	Baseline
2	Nano-SBS 1200 nm	30.77	19
3	Nano-SBS 455 nm	32.19	23
4	Nano-SBS 81 nm	36.39	32

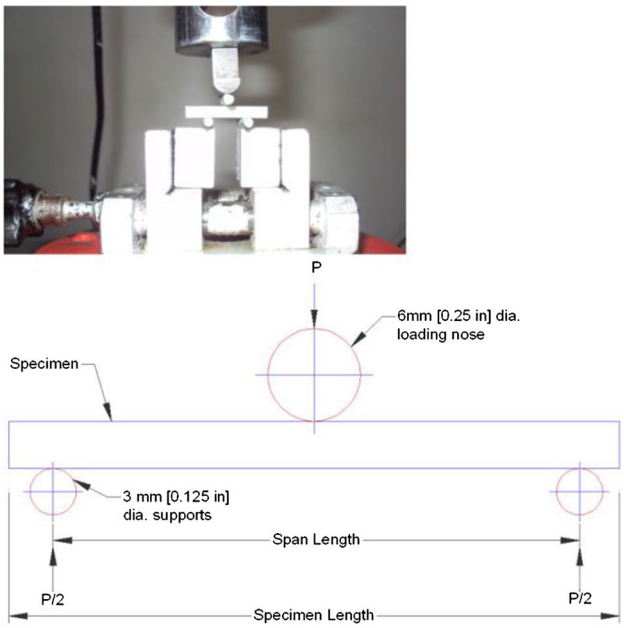

Fig. 23 SBS Setup and specimen configuration for short beams shear strength (ASTM D 2344)

HSBSNano: Hand mold coupons with nylon 6,6 nanofibers
VSBSNeat: VARTM coupons without nylon 6,6 nanofibers
VSBSNano: VARTM coupons with nylon 6,6 nanofibers
VModifySBSNano: Modified VARTM coupons with nylon 6,6 nanofibers (ModifySBSNano represents a nanocomposite with nylon 6,6 nanofibers and resins at the interface incorporated prior to VARTM).

The parameters such as F_{sbs}, P_m, b, and h are used to express the short beam shear strength (MPa), maximum load (N), breadth of the panel (mm), and thickness of the panel (mm), respectively. The tensile and bending strengths are compared for VARTM against hand molding. However, the mechanical characteristics of three-phase composites with interleaved nylon 6,6 nanofibers (1% by weight of neat composite) and a diameter of 1200 nm. In terms of short beam shear (SBS) strength, nanocomposites containing interleaved nylon 6,6 nanofibers with a diameter of 81 nm had the highest shear strength between laminate planes (ILSS). To assure uniqueness in the situation, the findings of the current studies are compared to those of a few study articles [33, 34] (Table 19). Delamination is the most frequent failure mode in laminated composite materials and it may cause catastrophic failure in critical engineering structures. The ways to prevent this failure is to toughen the crack against initiation and propagation. Matrix is weakest part in composite. It is brittle in nature which gets crack very easily. To toughen this crack the nanofibers are interleaved, which will try to due to high surface to volume ration it will try to toughen the matrix, which will result to transfer the load in between glass fibers.

Mode I: Fracture Toughness ASTM D 5528

The enhancement in mode I fracture toughness (Tables 20 and 21) attained by utilizing interleaved nylon 6,6 nanofibers in E-glass 7781 eight-shaft satin weave fabric is the most significant contribution of the research endeavor. Figure 24 depicts the specifics of an ASTM 5528 specimen, while Fig. 25 depicts the actual setup at Praj Laboratory. For the preparation of DCB coupons, ten laminas are chosen. Teflon film, with a thickness of no more than 13 microns, is applied after five laminas measuring 101.6 mm in length and 25.4 mm in width are laid. 25.4 mm is used for trimming, 25.4 mm is the length of the piano hinge tab, and 50.8 mm is the length of the actual crack opening. The ASTM-recommended dimensions are as follows:

Specimen length = 177.8 mm
Sample width = 25.4 mm
Specimen length of piano hinge = 25.4 mm
Crack length to be opened = 50.8 mm, specimen thickness = 2 to 3 mm.

Table 19 Comparison of results

1.	**Kumar et al. (2017) [33]** Flexural strength of electrospun nylon 6 fiber/E-glass fiber reinforced composites Hand lay-up method with nanofibers volume ratio (*2%* v/v) **Flexural strength** ***83.33 MPa*** (with the increase in nanofiber ratio, flexural strength is increased)		**Present flexural strength using glass molding (Table 4)** ***88.33 MPa*** (Epolam 5015 with *5%* weight of nylon 6,6 nanofibers having diameter *1200 nm*)
	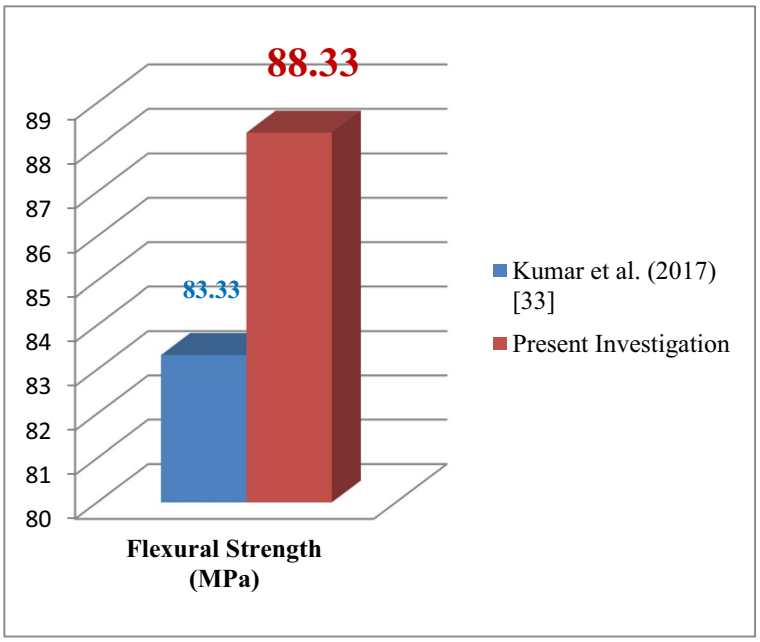		
2.	**Kumar et al. (2017) [33]** Flexural strength of electrospun nylon 6 fiber/E-glass fiber reinforced composites Hand lay-up method with nanofibers volume ratio (*2%* v/v)	**Tensile strength** ***152.9 MPa*** (with the increase in nanofiber ratio, tensile strength is increased)	**Present tensile strength using VARTM (Table 3)** ***520 MPa*** (E-glass fiber 7781 and Epolam 5015; Material System IV-without nanofibers)
	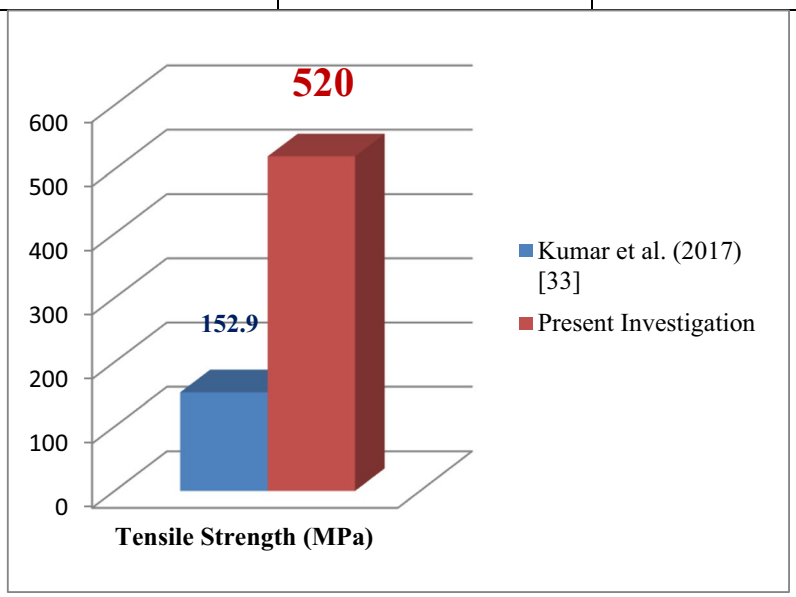		

Table 19 (continued)

3.	**Akkapeddi et al. (2000) [34]** Flexural strength of polyamide-6 (prepared via melt compounding technique) reinforced nanocomposites Polyamide-6 (PA-6)/NC having *4%* nanoclay **Flexural strength** ***152 MPa***		**Present flexural strength using glass molding (Table 4)** ***88.33 MPa*** (Epolam 5015 with *5%* weight of nylon 6,6 nanofibers having diameter *1200 nm*)
	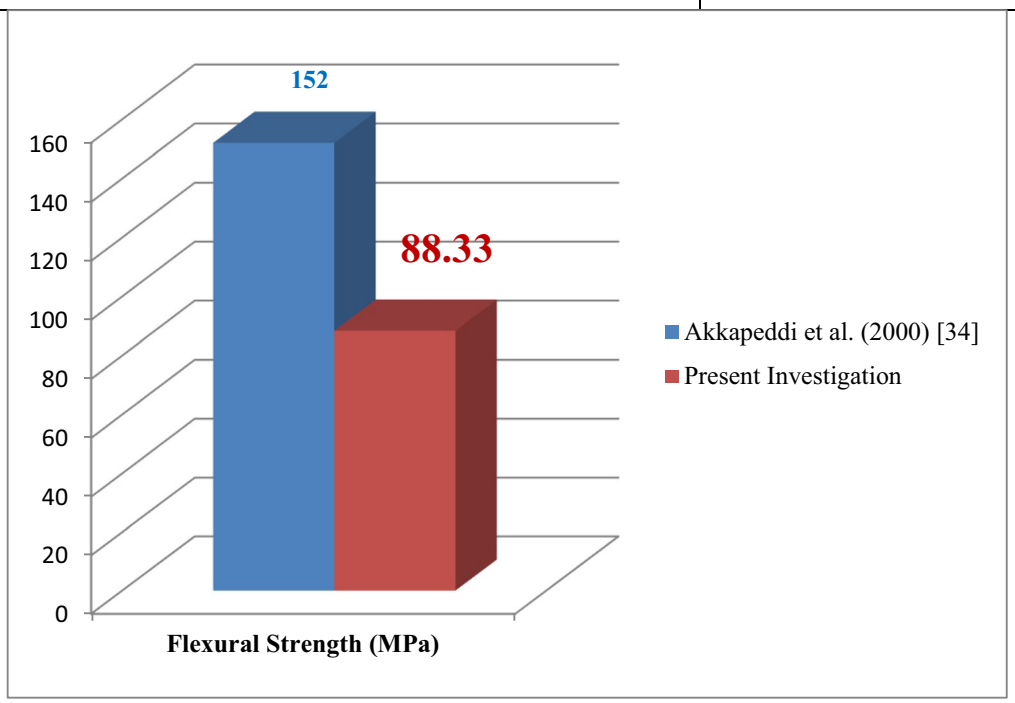		
4.	**Akkapeddi et al. (2000) [34]** Flexural strength of polyamide-6 (prepared via melt compounding technique) reinforced nanocomposites Polyamide-6 (PA-6)/NC having *4%* nanoclay	**Tensile strength** ***98 MPa***	**Present tensile strength using VARTM (Table 3)** ***520 MPa*** (E-glass fiber 7781 and Epolam 5015; Material System IV-without nanofibers)
	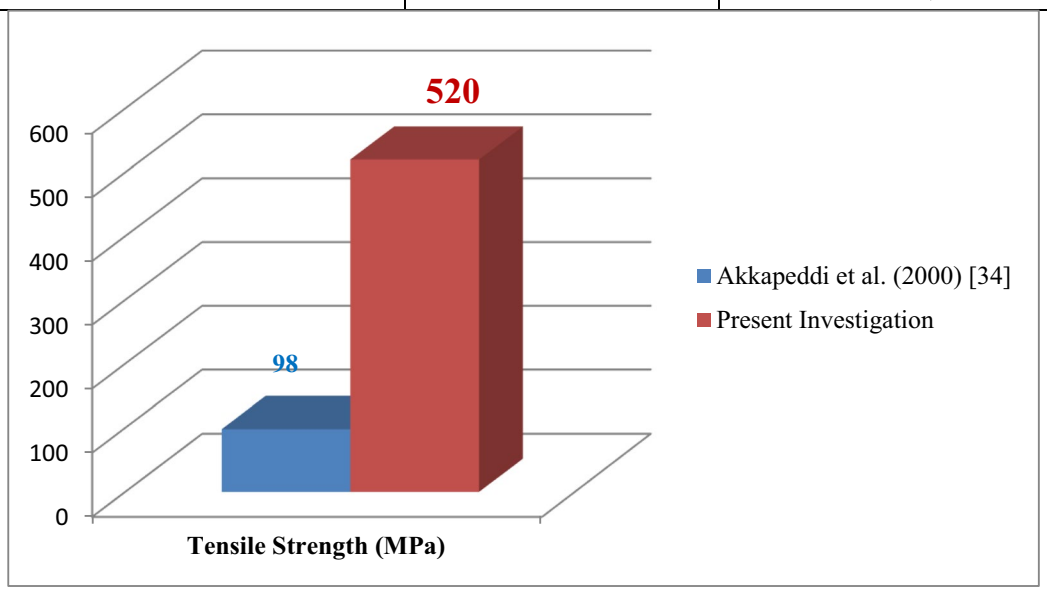		

Table 20 Sample computations of G_{IC} for a specimen of 0.5 Gms

Sr. no	a (m)	P (N)	COD (m)	G_{IC} (J/m^2)
1	0.001	17.93	0.053	20.29
2	0.002	22.14	0.054	49.2
3	0.003	26.26	0.055	85.94
4	0.004	29.98	0.056	128.48
5	0.005	33.32	0.057	175.36
6	0.010	47.62	0.062	460.95
7	0.015	50.56	0.067	679.15
8	0.020	41.94	0.072	699.06
9	0.025	35.50	0.077	691.55
10	0.030	27.34	0.082	600.40
	Width 'b' = 0.025			
Mean				359
Standard deviation				123.33

Table 21 Comparison of average G_{IC} values

Specimens	Neat (J/m^2)	Espun 1200 nm (J/m^2)	Espun 455 nm (J/m^2)	Espun 81 nm (J/m^2)
1	359	470.78	505.45	610
2	345	476.78	512	590
3	357.89	480	509	598
4	360.54	469.90	514.5	595
5	367.89	471	509.05	587
Avg. G_{IC}	358	473.69	510	596
Enhancement (%)		24%	29.80%	39.93%

With 1.02 mm five divisions and 5.08 mm extra five divisions, the white out is shown. The force is applied at one end of the hinge. At the indicated divide, the loads are reported. It is important to understand the rate of fracture propagation at the interlaminar contact, which is affected by cross-head movement speed. In order to examine the interaction of nanofibers, the cross-head movement speed of 12.7 mm/min is used. The test is completed after the load value has been decreased to 30% of the maximum load or the 50.8 mm fracture opening displacement has been achieved.

The application of load must be discontinued when the crack opening displacement (COD) reaches 50.8 mm or the load value reduces to 30% of the maximum load. Finally, the G_{IC}, or Mode I interlaminar fracture toughness is computed using the modified beam theory (MBT) technique as shown in Eq. (5).

$$G_{IC} = \frac{3 \times P \times \delta}{2 \times b \times a} \tag{5}$$

where P = applied force (N), δ = displacement of the load point (m), b = sample width (m), a = crack (delamination) length (m), G_{IC} = Mode I interlaminar fracture toughness (kJ/m^2), sample calculation of G_{IC} for a specimen is given in Tables 20 and 21.

Finite Element Analyses

Ansys 15 version is used to model (coupons for three-phase composites as per ASTM D 2344 using the unit cell method and two-phase composites-flexural strength, plagues as per ASTM D 790) and analyze the short beam shear (SBS) strengths in terms of shear stresses. The glass fabric 7781 with eight-shaft satin weave patterns with epoxy (Epolam 5015) is modeled using warp and weft properties for three-phase composites. Nanocomposites with interleaved nylon 6,6 nanofibers (having diameters such as 81, 455, and 1200 nm) as secondary reinforcement is modeled and analyzed for normal stresses and shear stresses. The material properties of the E-glass fibers and epoxy resins are considered from specification sheets provided by the manufacturers of E-glass fibers and epoxy resins (Table 22).

The model of basic elements is created according to the dimensions taken from the reference of ASTM D 2344, such as $X_1 = 0; X_2 = 2; Y_1 = 0; Y_2 = 0.3; Z_1 = 0; Z_2 = 2$. The properties of the materials, which are entered previously in the Ansys, are allotted to the elements. The element numbers 1, 4, 6, and 7 are wraps, so the properties of *material 1* are allotted to them. The element numbers 2, 3, 5, and 8 are wefts, so the properties of *material 2* are allotted to them. The merging of the nodes is required as the beam is created by copying the unit cell several times. Furthermore, nodes in the unit cell are still independent, so merging of the nodes with the close tolerance of 0.001 is done. To model the nanocomposite, an additional lamina of nylon 6,6 is layered at the interface and the same steps are followed until the tolerance 0.001 is achieved. The nanocomposite model is shown in Fig. 26. The boundary conditions are defined as displacements such as $U_X = U_Y = U_Z = 0$, and loading conditions are specified with a load such as $F_Y = -800$ N. After applying the load of 800 N, 30.51 MPa (shear stress) is developed in the neat composite beam. Similarly, the analyses of nanocomposite beams of SBS with nylon 6,6 with diameters of 1200, 455, and 81 nm (Fig. 27) and corresponding shear stresses are listed in Table 22. FEM analysis is done to study the significance of the nanofibers in two-phase composite with different diameter length scale and for different loads. The neat Epolam 5015 and Epolam 5015 with nylon 6,6 electrospun nanofibers specimens are prepared as per ASTM D 790-2003 for the analysis of flexural strength. The FEM models are analyzed under loads such as 90, 120, and 150 N loads acting on thicknesses such as 0.1, 0.2, and 0.3 mm, respectively (Table 22) as shown in Figs. 28 and 29.

In the case of two-phase composite (manufactured using glass molding), the nanofibers having diameters 81 nm diameter) are showing comparatively good strength as compared to the nanofibers with 455 and 1200 nm diameters. Here, the authors also observed that with the thickness in percentage of nanofibers, the strength is increased. In the case of three-phase composite, the shear stress in SBS coupon with nylon

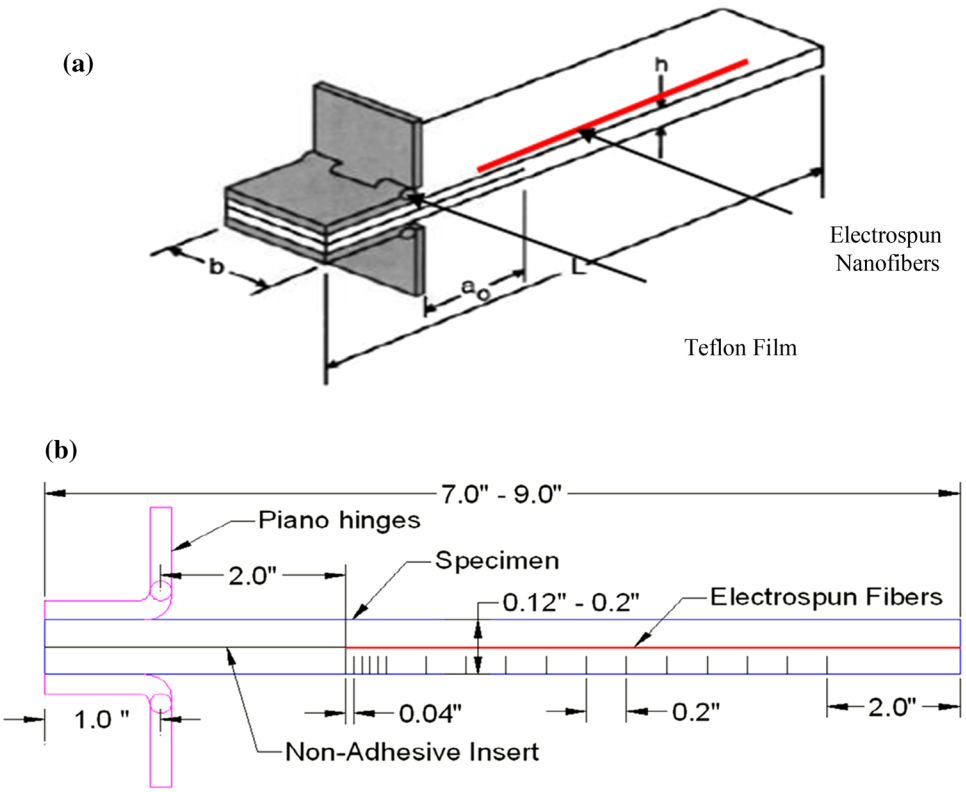

Fig. 24 Double cantilever beam test

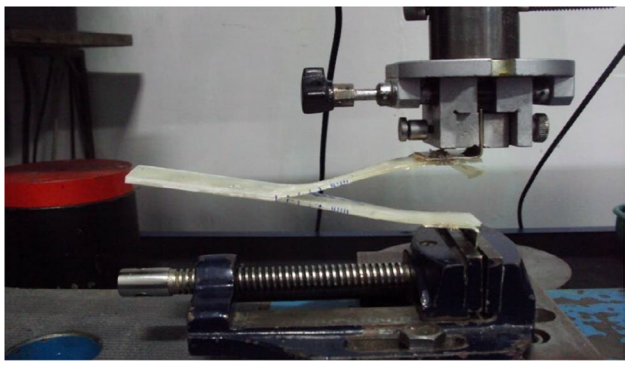

Fig. 25 Praj Lab's (India) double cantilever beam test specimens

6,6 nanofibers (having 81 nm diameter) is less. Finally, it is concluded that the finite element method (FEM) is a promising concept to understand the behavior of the nanocomposite materials. The woven composite unit cell model was established to investigate the interactions between the warp and weft. The shear stress in the neat composite is 30.50 MPa using 1000 N load. The shear stresses in SBS coupons with nylon 6,6 nanofibers [35–39] having diameters such as 1200, 455, and 81 nm are 40.134, 43.281, and 47.724 MPa, respectively. The enhancements in resisting shear stresses (as compared to neat composites) of around 24, 30, and 36% are observed in the nanocomposites, after the addition of nanofibers of diameters 1200 nm (1% of this diameter), 455, and 81 nm, respectively. For each panel, five samples were tested. Various alternatives were tried so as to remove the voids, by heating glass mold, changing the glass mold with aluminum plate, which showed some enhancement but without maintaining the consistency. Due to the manufacturing limitations, the finite element method has been used for the validation of the multiscale effect of the nylon 6,6 nanofibers reinforced in three-phase nanocomposite as discussed in manuscript.

Conclusions

Manufacturing Method

Manufacturing of E-glass fiber reinforced epoxy nanocomposites with interleaved nylon 6,6 nanofibers, it is found that hand molding could be the cost-effective method and comparatively easy to operate; however, unevenness in the thickness became the limitation of the method. Also, it was observed large amounts of voids which are entrapped into the composites using the method, thereby the quality and mechanical performance are deteriorated. VARTM, on the other hand, is used to fabricate composites (uniform thickness and less porosity) with improved mechanical properties. Its cost is less as compared to the resin transfer molding (RTM) due to the replacement of one mold by plastic bagging. VARTM also offered a good fiber weight fraction (in the present case it is around 63%) as compared to other processes and thus resulting in improved mechanical strength. To justify the same, four different material systems (I, II, III, and IV) were

Table 22 Material properties and results of finite element analysis

A. Material properties of E-glass fibers 7781/epoxy (Epolam 5015) composites

Warp (Material 1)	Weft (Material 2)
$E_X = 19 \times 10^9$,$E_Y = 4.75 \times 10^9$, $E_Z = 4.75 \times 10^9$	$E_X = 4.75 \times 10^9$, $E_Y = 19 \times 10^9$, $E_Z = 19 \times 10^9$
$\nu_{XY} = 0.245$,$\nu_{YZ} = 0.36$,$\nu_{XZ} = 0.245$	$\nu_{XY} = 0.36$, $\nu_{YZ} = 0.245$, $\nu_{XZ} = 0.36$
$G_{XY} = 2430$,$G_{YZ} = 1958$,$G_{XZ} = 2430$	$G_{XY} = 2430$,$G_{YZ} = 2430$, $G_{XZ} = 1958$
*The third material is nylon 6,6 nanofibers ($E_X = 4 \times 10^9$, and $\nu_{XY} = 0.39$)	

B. SBS results for neat and nanocomposite panels using finite element analysis under 1000 N Load

Sr. no	Diameter	τ_{XY}(MPa)
1	SBS (Neat panel)	30.50
2	SBS panel (nylon 6,6 nanofibers having diameter 1200 nm)	40.134
3	SBS panel (nylon 6,6 nanofibers having diameter 455 nm)	43.281
4	SBS panel (nylon 6,6 nanofibers having diameter 81 nm)	47.724

C. Value of stresses for neat panels and panels with nanofibers (having diameters such as 1200, 455, and 81 nm under different loads such as 90, 120, and 160 N, respectively)

Load (N)	Stress (MPa) Neat Panel	Stress (MPa) 1200 nm	Stress (MPa) 455 nm	Stress (MPa) 81 nm
90	42.61	40.59	39.67	36.54
120	56.82	46.12	45.78	42.68
160	75.76	61.49	61.40	60.55

D. Value of stresses for neat panels and panels with nanofibers (having diameters such as 1200 nm under different loads such as 90, 120, and 160 N, respectively)

Load (N)	Stress (MPa) Neat Panel	Stress (MPa) 1200 nm with 0.1 mm thickness	Stress (MPa) 1200 nm with 0.2 mm thickness	Stress (MPa) 1200 nm with 0.3 mm thickness
90	42.61	34.59	30.12	26.40
120	56.82	46.12	40.16	34.88
160	75.76	61.49	53.55	45.50

characterized for tensile strength and flexural strength. It is observed that (a) material systems I are showing an increase in tensile and flexural strength by 20% and 36%, respectively; (b) material systems II are showing an increase in tensile and flexural strength by 17.5% and 18%, respectively; (c) material systems III are showing an increase in tensile strength by 18.6%; (d) material systems IV are showing improvement in tensile and flexural strength by 21.7% and 42%, respectively.

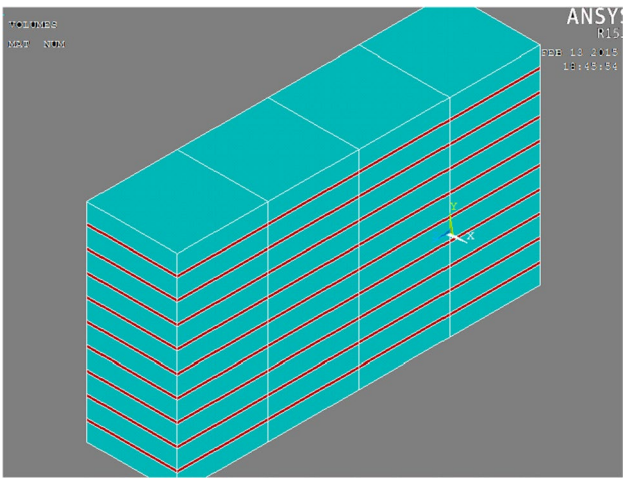

Fig. 26 SBS model with nylon 6,6 interface layer

Electrospinning

The design of experiment is performed for nylon 6,6 nanofibers by using tools such as full factorial design and Taguchi. The influences of control parameters such as the nozzle of spinneret to grounded collector distance, rate of flow, high-voltage power supply and concentration of the polymeric solution are carefully studied. The optimum diameter of 360 nm for nylon 6,6 is synthesized using the optimized methodology—Design of experiment with the following parameters: distance 15 cm, voltage 15 kV, and flow rate 0.2 mL/h (Full factorial). The optimized diameter of 81 nm by the Taguchi method is synthesized following the optimized setting of a polymeric solution having 20% nylon 6,6

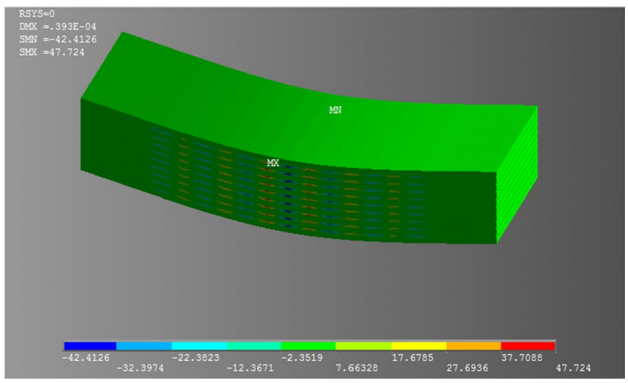

Fig. 27 FEM model of SBS shear stress with nylon 6,6 nanofibers having diameter 81 nm in deformed condition

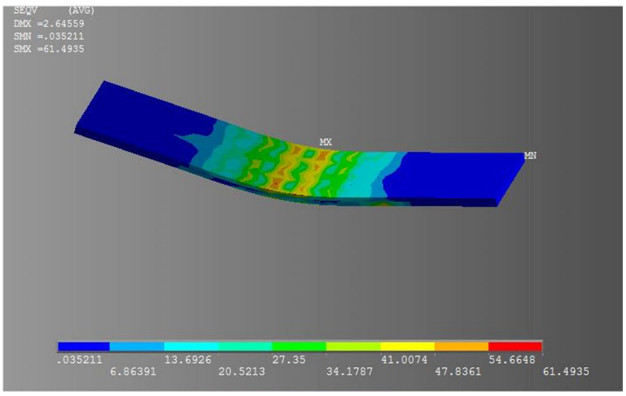

Fig. 28 0.1-mm-thick layer of Epolam 5015 with nylon 6,6 nanofibers having diameter 1200 nm under 160 N load

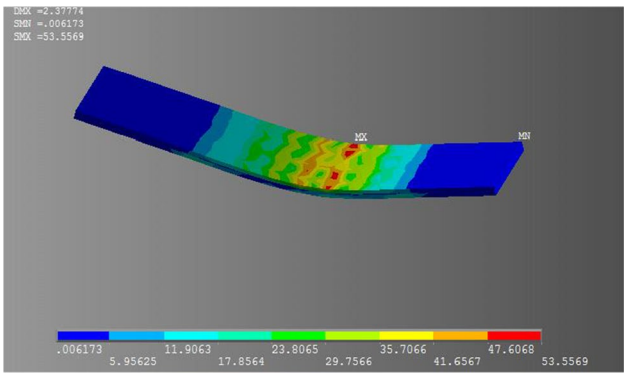

Fig. 29 0.2-mm-thick layer of Epolam 5015 with nylon 6,6 nanofibers having diameter 1200 nm under 160 N load

in 10 mL of 98% HCCOH with the electrospinning unit having a high-voltage of 25 kV, the nozzle to the spinneret to grounded collector distance of 20 cm, and a flow rate of 0.2 mL/h and speed of grounded cylindrical collector around 1000 rpm. Electrospun nanofibers with ultrathin 81 nm diameters are investigated to be the smallest in their range so far. The nanofibers (prepared via Taguchi with diameters of 1200, 455, and 81 nm) are used to fabricate nylon 6,6 nanofibers interleaved E-glass fiber reinforced epoxy nanocomposites to validate the study goal.

Glass Molding (Two-Phase Composite)

Two-phase nanocomposites having uniform thickness could be fabricated using a glass molding process with less indentation marks. On the other hand, deterioration in the above mechanical properties is noted in the case of specimens having 1200 nm diameter of electrospun nylon 6,6 nanofibers due to the formation of voids during the glass molding process.

Furthermore, two-phase plagues are studied for which the experimental results are not found satisfactory under different loads and for various thicknesses of composites reinforced with nylon 6,6 nanofibers and it has been concluded that it had happened due to manufacturing problems which are unavoidable in the present conditions, so far. So FEA model is developed for two-phase composite with nylon 6,6 nanofibers of diameters 81 nm, is found to have improved strength as compared to those with nylon 6,6 nanofibers of diameters 1200 and 455 nm.

Short Beam Shear Strength (ILSS) Three-Phase Composite

To investigate the strengths of E-glass fiber reinforced epoxy nanocomposites with interleaved nylon 6,6 nanofibers, ASTM D 2344 of shear strength between laminate planes (ILSS) of short beam specimens. The present investigations aim to improve the shear strength between laminate planes (ILSS) of E-glass and Epolam 5015 composite laminates by interleaving electrospun nylon 6,6 nanofibers of various diameters at the interfaces between fibers and matrix. Improved shear strength between laminate planes (ILSS) (such as short beam shear (SBS) strength) is observed in nylon 6,6 nanofibers (diameter 81 nm) reinforced composites. The short beam shear (SBS) strength of nylon 6,6 nanofibers interleaved E-glass fiber reinforced epoxy nanocomposites could be improved by 24, 30, and 36% after adding 1% nylon 6,6 diameters of 1200, 455, and 81 nm, respectively, according to finite element analysis (as compared to neat composites).

The results are conceptualized using the finite element method. The unit cells are preferred to analyze the SBS specimens as per ASTM standards for simulation studies. The shear stresses are found to be around 30.50, 40.134, 43.281, and 47.724 MPa for neat composite, composite with nylon 6,6 nanofibers of 1200 nm diameter, 455 and 81 nm diameters, respectively.

Fracture Toughness (Three-Phase Composite)

Glass Epoxy composite with nylon 6,6 nanofiber (1 gm) as interface at critical ply with 1.2 μm, 445 nm, and 81 nm nanofiber diameters showed enhancement in fracture toughness by 24, 30, and 40%, respectively. The small nanofiber diameters are preferred to increase the energy absorbing capability of the laminate.

Funding The authors have not been funded in any way to carry out the research activities.

Declarations

Conflict of interest The authors declare that there are no conflicts of interest.

Appendix I: Properties of Glass Fiber 7781

interglas

GLASS FILAMENT FABRICS for PLASTICS REINFORCEMENT

PRODUCT SPECIFICATION

	Unit	Standard	CS-ITG	Tolerance	Specification
Style Number		**92626**		**/ FK100**	
Tensile strength					DIN EN 2747
warp	MPa	335		± 10%	
weft	MPa	320		± 10%	
Young's-Modulus					
warp	GPa	19		± 10%	
weft	GPa	18		± 10%	
Compression strength					DIN 53454
warp	MPa	375		± 10%	DIN 65380
weft	MPa	360		± 10%	DIN prEN 2580
Compression-Modulus					
warp	GPa			± 10%	
weft	GPa			± 10%	
Interlaminar shear strength					DIN EN 2377
warp	MPa	50		± 10%	
weft	MPa	45		± 10%	
Flexural strength					DIN EN 2746
warp	MPa	495		± 10%	
weft	MPa	460		± 10%	
Flexural-Modulus					
warp	GPa	17		± 10%	
weft	GPa	17		± 10%	

Remarks

1) Temperature resistance for dry fabrics

INTERGLAS Technologies AG, Benzstraße 14, D-89155 Erbach, Telefon +49 (0)7305 / 955-416, Fax +49 (0)7305 / 955-512

TS / 07/03/2008

Page 2 of 2

Appendix II: Properties of Epoxy Epolam5015

Epolam 5015 Resin

Technical Data Sheet

Epolam 5014 – 5015 – 5016 Hardeners

Laminating system for resin infusion

Tg 176°F (80°C) – Gel times 45 minutes to 4 hours

Description

Epolam 5015 resin is a low-viscosity system designed for resin infusion and offered with a choice of three different speed hardeners. This allows the selection of a pot life suitable to the size of the part being produced.

Applications

- *Production of composite parts by resin infusion methods*
- *Suitable for vacuum-bagging, RTM and filament winding*

Properties

- *Lloyd's Register of London approved for the construction of marine vessels*
- *Very low viscosity*
- *Readily wets out fabrics*
- *Good mechanical properties*
- *Good wetting of core materials such as balsa wood and foam*
- *Suitable for marine applications*

Physical Properties

		Epolam 5015 Resin	Epolam 5014 Hardener	Epolam 5015 Hardener	Epolam 5016 Hardener
Composition		Epoxy	Amine	Amine	Amine
Mix Ratio, by weight		100	34	30	36
Appearance		Liquid	Liquid	Liquid	Liquid
Color		Light amber	Light amber	Colorless	Light amber
Viscosity @ 77°F (25°C) mPa.s	Brookfield LVT	800	20	12	20
Density @ 77°F (25°C) (g/cc)	ISO 1675:1985	1.15	0.94	0.94	0.94
Viscosity, mixed @ 77°F (25°C) mPa.s	Brookfield LVT		225	210	225
Pot life, 500g at 77°F (25°C)			45 minutes	135 minutes	225 minutes
Cured density @ 74°F (23°C) (g/cm^3)	ISO 2781: 1985		1.12	1.10	1.12

PROCESSING

Caution: EPOLAM 5015 system must be cured (2 hrs at 122°F (50°C) at least) to be demolded.
To obtain the desired temperature resistance and the optimal mechanical properties it is necessary to postcure the EPOLAM 5015 system. This step takes place 24 to 48 hours after application depending on the hardener. In order to avoid any distortion risks it is recommended to support the part on a frame before curing.
To allow a good beginning of polymerization of EPOLAM 5015/5016 system it is recommended to work at 68°F (20°C) minimum.
For any further information concerning the Resin Infusion Method and ancillary products provided by Axson, please contact our Technical Support Department.

AXSON NA USA
1611 Hults Drive
Eaton Rapids, MI
48827
Tel. (517) 663-8191
Fax (517) 663-0523
Email : info@axson-na.com

AXSON GmbH
Dietzenbach
Tél. (++49) 60 74 407110

AXSON Italie
Saronno
Tel. (++39) 02 96 70 23 36

AXSON IBERICA
Barcelona
Tel. (++34) 93 225 16 20

AXSON UK Limited
Newmarket
Tel. (++44) 1638 660 062

AXSON BRASIL
Sao Paulo
Tel. (++55) 11 5687 7331

AXSON MEXICO
Mexico DF
Tel. (++52) 55 5264 49 22

AXSON SHANGHAI
Shanghai
Tel. (++86)-58 68 30 37

AXSON France
Cergy
Tél. (++33) 1 34 40 34 60
Email : axson@axson.fr

AXSON JAPAN
OKAZAKI CITY
Tel.(++81) 564 26 2591

Appendix III: EPON-862 Resin Properties

AXSON TECHNOLOGIES

Epolam 5015 Resin

Technical Data Sheet

Epolam 5014 – 5015 – 5016 Hardeners

Laminating system for resin infusion

Tg 176°F (80°C) – Gel times 45 minutes to 4 hours

Cured Properties at 74°F (23°F) [1]					
Epolam 5015 Resin with			Epolam 5014 Hardener	Epolam 5015 Hardener	Epolam 5016 Hardener
Glass Transition Temperature (Tg) • 7 days at room temperature • 16 hours at 122°F (50°C) • 16 hours at 176°F (80°C)	D.S.C. - Mettler	°F (°C)	 106 (41) 160 (71) 176 (80)	 104 (40) 158 (70) 180 (82)	 108 (42) 140 (60) 178 (81)
Hardness	ASTM D-2240	Shore D	85	85	85
Tensile Strength	ASTM D638	psi (MPa)	10,100 (70)	11,600 (80)	10,100 (70)
Elongation at break	ASTM D638	%	7	6	8
Flexural Strength	ASTM D790	psi (MPa)	14,500 (100)	15,200 (105)	13,800 (95)
Flexural Modulus	ASTM D790	psi (MPa)	421,000 (2,900)	435,000 (3,000)	406,000 (2,800)

[1]Average values on laboratory prepared test samples of neat (unreinforced) resin, 24 hours at room temperature plus 16 hours at 176°F (80°C)

Storage Conditions

This product has a shelf life of 24 months as indicated by the expiration date on the container when stored in original unopened containers between 59 – 77°F (15 – 25°C). Any opened can must be tightly closed.

Handling Precautions

Normal health and safety precautions should be observed when handling these products :

- *Ensure good ventilation*
- *Wear gloves, and safety glasses*

For further information, please consult the material safety data sheet.

Guarantee

The information contained in this technical data sheet results from research and tests conducted in our Laboratories under precise conditions. It is the responsibility of the user to determine the suitability of AXSON products, under their own conditions before commencing with the proposed application. AXSON guarantees the conformity of their products with their specifications but cannot guarantee the compatibility of a product with any particular application. AXSON disclaims all responsibility for damage from any incident which results from the use of these products. The responsibility of AXSON is strictly limited to reimbursement or replacement of products which do not comply with the published specifications.

AXSON NA USA
1611 Hults Drive
Eaton Rapids, MI
48827
Tel. (517) 663-8191
Fax (517) 663-0523
Email : info@axson-na.com

AXSON GmbH
Dietzenbach
Tél. (++49) 60 74 407110

AXSON Italie
Saronno
Tel. (++39) 02 96 70 23 36

AXSON IBERICA
Barcelona
Tel. (++34) 93 225 16 20

AXSON UK Limited
Newmarket
Tel. (++44) 1638 660 062

AXSON BRASIL
Sao Paulo
Tel. (++55) 11 5687 7331

AXSON MEXICO
Mexico DF
Tel. (++52) 55 5264 49 22

AXSON SHANGHAI
Shanghai
Tel. (++86)-58 68 30 37

AXSON France
Cergy
Tél. (++33) 1 34 40 34 60
Email : axson@axson.fr

AXSON JAPAN
OKAZAKI CITY
Tel.(++81) 564 26 2591

HEXION
Specialty Chemicals

Technical Data Sheet

Re-issued March 2005

EPON™ Resin 862

Product Description

EPON™ Resin 862 (Diglycidyl Ether of Bisphenol F) is a low viscosity, liquid epoxy resin manufactured from epichlorohydrin and Bisphenol-F. This resin contains no diluents or modifiers. EPON Resin 862 may be used as the sole epoxy resin or combined with other resins such as EPON Resin 828. When blended with EPON Resin 828, EPON Resin 862 provides a technique to reduce viscosity with no sacrifice in chemical and solvent resistance properties, and the blended resin will exhibit improved crystallization resistance properties when compared to the neat, liquid, Bisphenol-A or Bisphenol-F type resins. When EPON Resin 862 is cross-linked with appropriate curing agents, superior mechanical, adhesive, electrical and chemical resistance properties can be obtained.

Application Areas/Suggested Uses

- Solventless or high solids/low VOC maintenance and marine coatings
- Chemical resistant tank linings, floorings, and grouts
- Fiber reinforced pipes, tanks, and composites
- Tooling, casting, and molding compounds
- Construction, electrical, and aerospace adhesives

Benefits

- Low viscosity
- Low color
- Reacts with a full range of epoxy curatives
- Good balance of mechanical, adhesive, and electrical properties
- Good chemical resistance
- Superior physical properties vs. diluted (6 Poise) resins

Sales Specification

Property	Units	Value	Test Method/Standard
Weight per Epoxide	g/eq	165 – 173	ASTM D1652
Viscosity at 25°C	P	25 – 45	ASTM D445
Color	Pt-Co	200 max.	ASTM D1209

Typical Properties

EPON Resin 862

Property	Units	Value	Test Method/Standard
Density at 25°C	lb/gal	9.8	ASTM D1475

Processing/How to use

General Information

Chemical Identification and Classification

- Chemical Abstract Service Registry Number: 28064-14-4 (EPA/TSCA Inventory designation)
- Chemical designation: Bisphenol-F/epichlorohydrin epoxy resin

Chemical Structure (ideal)

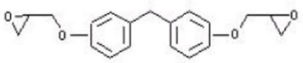

Benefits of Using EPON Resin 862

- Reduced diluent levels to achieve specific viscosity targets
- Higher solids or reduced solvent levels for coatings
- Improved handling and flow in colder application environments
- Improved fiber and filler wetting

Crystallization Resistance

Figure 1 / **Crystallinity Rating of Epoxy Resins** Under **Accelerated Testing**[1]

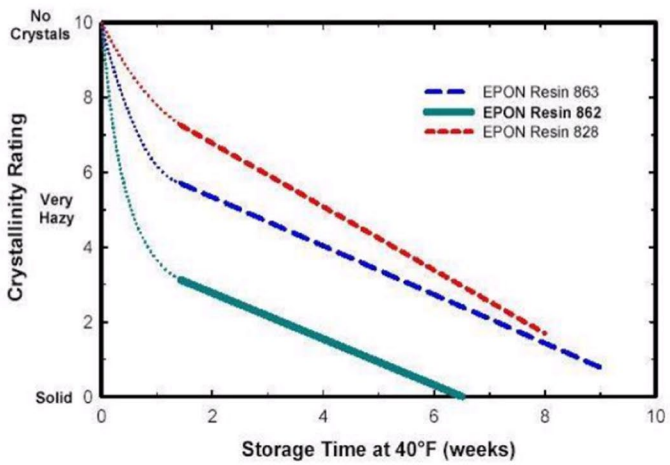

[1] RPP test method SMS 2018 (diluted to 6 Poise and seeded with epoxy crystals

EPON Resin 862

Crystallization of BPF epoxy resins is possible in the temperature range between the glass transition point (-10 to -20°C/14 to -4°F) and the general melting range (typically 30 to 60°C/86 to 140°F). BPF resins modified with HELOXY Modifiers 7, 8, and 61 show a greater tendency to crystallize and should not be stored cold. If aromatic modifiers are acceptable, HELOXY Modifier 62 (Cresyl Glycidyl Ether) has been shown to give more resistance to crystallization than the aliphatic HELOXY Modifiers.
In general, the crystallization behavior for EPON Resin 862 follows these trends:

- EPON Resin 828 and EPON Resin 863 have better crystallization resistance than EPON Resin 862.
- The crystallization resistance of EPON Resin 862 is generally better than standard BPA epoxy (EPON Resin 828) when diluted to equivalent viscosities.
- The crystallization resistance of the unmodified BPA epoxy is retained when blended with EPON Resin 862 or EPON Resin 863 for reduced viscosity.

For BPF resins that have crystallized, heat the tank, drum, or pail contents to 140 to 150°F (60 to 66°C) until all visual evidence of crystallization is gone. All associated piping, pumps, etc. also needs to see this heat exposure to remove any crystals from the system that could nucleate additional crystal growth. For heated storage, the lowest effective temperature should be used. When necessary to heat EPON Resin 862 for extended periods of time, it is recommended that an inert gas blanket the resin surface.

Viscosity Properties

Figure 2 / **Effect of Temperature on EPON Resin 862 and Blends with EPON Resin 828**

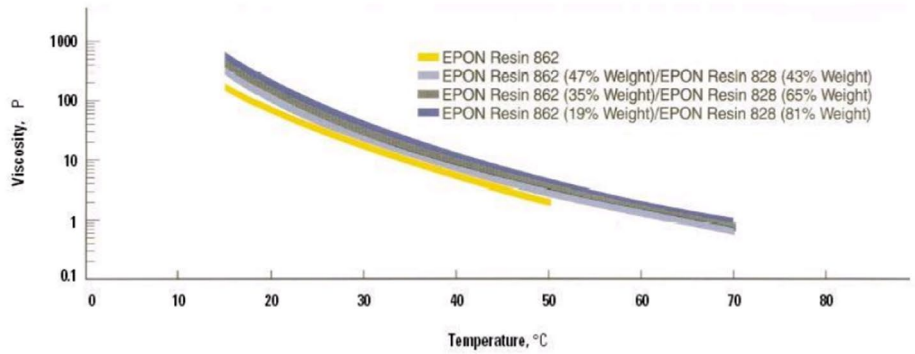

Figure 3 / **Viscosity of EPON Resin 862 / EPON Resin 828 Blends at 25°C**

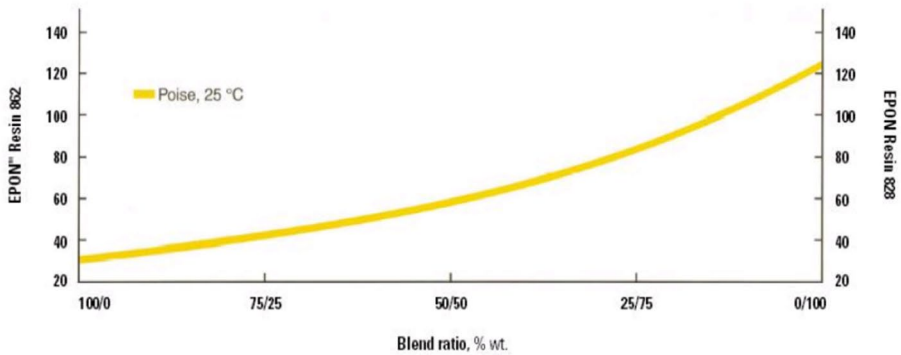

Figure 4 / **Viscosity of EPON Resin 862 / EPON Resin 155 Blends at 25°C**

EPON Resin 862

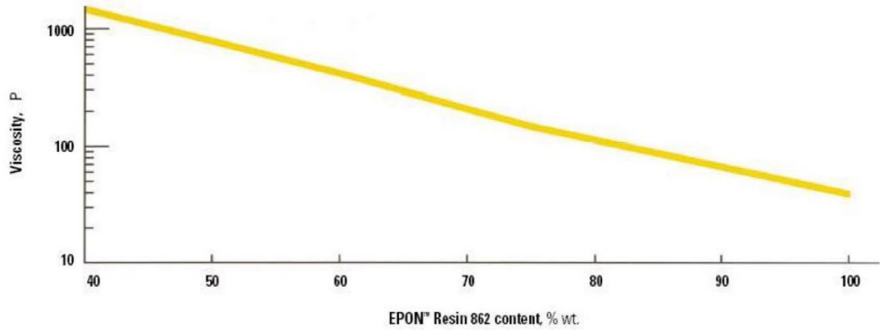

Figure 5 / **Viscosity of EPON Resin 862 and EPON Resin 828 at 25°C, when diluted with HELOXY Modifier 61**

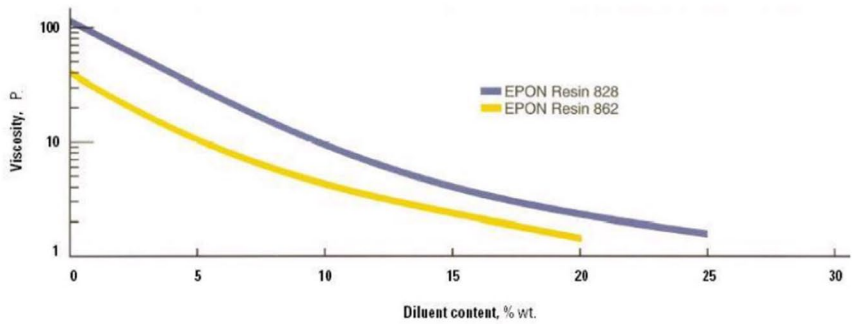

Figure 6 / **Viscosity of EPON Resin 862 and EPON Resin 828 at 25°C, when diluted with HELOXY Modifier 8**

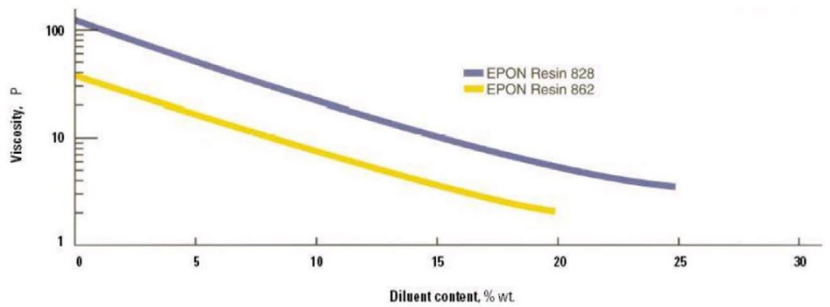

Safety, Storage & Handling

Please refer to the MSDS for the most current Safety and Handling information.

EPON Resin 862 should be stored in tightly sealed containers of metal, glass, or polyolefin plastic at normal room temperatures. If EPON Resin 862 develops haziness or crystallizes during storage, it can be restored to its original condition by gently warming the container and its contents to approximately 170-190°F until all visual evidence of crystallization is gone. Upon cooling to normal ambient temperature conditions, the product will regain its original liquid state physical properties. This process can be repeated as necessary.

Exposure to these materials should be minimized and avoided, if feasible, through the observance of proper precautions, use of appropriate engineering controls and proper personal protective clothing and equipment, and adherence to proper handling procedures. **None of these materials should be used, stored, or transported until the handling precautions and recommendations as stated in the Material Safety Data Sheet (MSDS) for these and all other products being used are understood by all persons who will work with them.** Questions and requests for information on Hexion Specialty Chemicals, Inc. ("Hexion") products should be directed to your Hexion sales representative, or the nearest Hexion sales office. Information and MSDSs on non-Hexion products should be obtained from the respective manufacturer.

Packaging
Available in bulk and drum quantities.

Contact Information
For product prices, availability, or order placement, call our toll-free customer service number at:
1-877-859-2800

For literature and technical assistance, visit our website at: www.hexion.com

® and ™ Licensed trademarks of Hexion Specialty Chemicals, Inc.

DISCLAIMER
The information provided herein was believed by Hexion Specialty Chemicals to be accurate at the time of preparation or prepared from sources believed to be reliable, but it is the responsibility of the user to investigate and understand other pertinent sources of information, to comply with all laws and procedures applicable to the safe handling and use of the product and to determine the suitability of the product for its intended use. **HEXION SPECIALTY CHEMICALS MAKES NO WARRANTY, EXPRESS OR IMPLIED, CONCERNING ANY PRODUCT OR THE MERCHANTABILITY OR FITNESS THEREOF FOR ANY PURPOSE OR CONCERNING THE ACCURACY OF ANY INFORMATION PROVIDED BY HEXION SPECIALTY CHEMICALS**, except that the product shall conform to contracted specifications, and that the product does not infringe any valid United States patent.

PDS-3950- (Rev.3/12/2010 10:35:21 AM)

References

1. R. Khajavi, M. Abbasipour, Electrospinning as a versatile method for fabricating core shell, hollow and porous nanofibers. Scientia Iranica Trans. F: Nanotechnol. **19**(6), 2029–2034 (2012). https://doi.org/10.1016/j.scient.2012.10.037
2. J.L. Skinner, J.M. Andriolo, J.P. Murphy, B.M. Ross, Electrospinning for nano- to mesoscale photonic structures. Nanophotonics **6**(5), 765–787 (2017). https://doi.org/10.1515/nanoph-2016-0142
3. J.-W. Lu, Y.-L. Zhu, Z.-X. Guo, P. Hu, J. Yu, Electrospinning of sodium alginate with poly(ethylene oxide). Polymer **47**(23), 8026–8031 (2006). https://doi.org/10.1016/j.polymer.2006.09.027
4. D.H. Reneker, I. Chun, Nanometer diameter fibers of polymer, produced by electrospinning. Nanotechnology **7**, 216–223 (1996)
5. F. Kayaci, H.S. Sen, E. Durgun, T. Uyar, Electrospun nylon 6,6 nanofibers functionalized with cyclodextrins for removal of toluene vapor. J. Appl. Polym. Sci. **132**(18), 41941 (2015). https://doi.org/10.1002/app.41941
6. M.R. Mousavi, M. Rafizadeh, F. Sharif, Investigation of effect of electrospinning parameters on morphology of polyacrylonitrile/polymethylmethacrylate nanofibers: A Box-Behnken-based study. J. Macromol. Sci. Part B Phys. **54**(8), 975–991 (2015). https://doi.org/10.1080/00222348.2015.1042628

7. S. Jiang, A. Greiner, S. Agarwal, Short nylon-6 nanofiber reinforced transparent and high modulus thermoplastic polymeric composites. Compos. Sci. Technol. **87**, 164–169 (2013). https://doi.org/10.1016/j.compscitech.2013.08.011
8. N.J. Kanu, E. Gupta, U.K. Vates, G.K. Singh, Electrospinning process parameters optimization for biofunctional curcumin/gelatin nanofibers. Mater. Res. Express. **3**, 035022 (2020). https://doi.org/10.1088/2053-1591/ab7f60
9. D.C. Montgomery, *Design and Analysis of Experiments*, 8th edn (John Wiley & Sons, 2014). ISBN 1621982270, 9781621982272.
10. J.R. Phillip, Taguchi techniques for quality engineering. McGraw-Hill Book Company **5**(3), 249 (1989). https://doi.org/10.1002/qre.4680050312
11. L. Huang, J. Mccutcheon, Hydrophilic nylon 6,6 nanofibers supported thin film composite membranes for engineered osmosis. J. Membr. Sci. **457**, 162–169 (2014). https://doi.org/10.1016/j.memsci.2014.01.040
12. C.-W. Lo, J.-X. Li, Lu. Ming-Chang, Frosting and defrosting on the hydrophilic nylon-6 nanofiber membrane–coated surfaces. Appl. Therm. Eng. **184**, 116300 (2021). https://doi.org/10.1016/j.applthermaleng.2020.116300
13. T.M. Subrahmanya, A.B. Arshad, P.T. Lin, J. Widakdo, H.K. Makari, F.M. Hannah, C.-C. Austria, J.-Y. Lai, W.-S. Hung, A review of recent progress in polymeric electrospun nanofiber membranes in addressing safe water global issues. RSC Adv. **11**, 9638–9663 (2021). https://doi.org/10.1039/d1ra00060h
14. A. Keirouz, N. Radacsi, Q. Ren, A. Dommann, G. Beldi, K. Maniura-Weber, R.M. Rossi, G. Fortunato, Nylon-6/chitosan core/shell antimicrobial nanofibers for the prevention of mesh-associated surgical site infection. J. Nanobiotechnology **18**, 51 (2020). https://doi.org/10.1186/s12951-020-00602-9
15. S.S. Chavan, K.M. Sinha, P.V. Londhe, Synthesis and characterization of composite nanofibers with VARTM and electrospinning process. Carbon Sci. Technol. **5**(3), 289–295 (2013)
16. M. Bulut, M. Alsaadi, A. Erkliğ, A comparative study on the interlaminar shear strength of S-glass/epoxy composites containing borax, perlite and sewage sludge ash particles. Mater. Res. Express **6**(9), 095330 (2019). https://doi.org/10.1088/2053-1591/ab3360
17. X. Niu, L. Wang, M. Xu, M. Qin, L. Zhao, W. Yan, Y. Hu, X. Lian, Z. Liang, S. Chen, W. Chen, D. Huang, Electrospun polyamide-6/chitosan nanofibers reinforced nano-hydroxyapatite/polyamide-6 composite bilayered membranes for guided bone regeneration. Carbohydr. Polym. **260**, 117769 (2021). https://doi.org/10.1016/j.carbpol.2021.117769
18. B. Li, S. Wei, H. Xuan, Y. Xue, H. Yuan, Tailoring fineness and content of nylon-6 nanofibers for reinforcing optically transparent poly(methyl methacrylate) composites. Polym. Compos. **42**(7), 3243–3252 (2021). https://doi.org/10.1002/pc.26054
19. I. Sriyanti, M.P. Agustini, J. Jauhari, S. Sukemi, Z. Nawawi, Electrospun nylon-6 nanofibers and their characteristics. Jurnal Ilmiah Pendidikan Fisika Al-BiRuNi **9**(1), 9–19 (2020). https://doi.org/10.24042/jipfalbiruni.v9i1.5747
20. S.S. Abdelhady, S.H. Zoalfakar, M.A. Agwa, A.A. Ali, Electrospinning process optimization for Nylon 6,6/Epoxy hybrid nanofibers by using Taguchi method. Mater. Res. Express **6**, 095314 (2019). https://doi.org/10.1088/2053-1591/ab3021
21. S.S. Abdelhady, S.H. Zoalfakar, M.A. Agwa, A.A. Ali, Mechanical and thermal characteristics of optimized electrospun nylon 6,6 nanofibers by using Taguchi method. NANO **14**(11), 1950 (2019). https://doi.org/10.1142/S179329201950139X
22. M.T. Aljarrah, N.R. Abdelal, Improvement of the mode I interlaminar fracture toughness of carbon fiber composite reinforced with electrospun nylon nanofiber. Compos. B Eng. **165**, 379–385 (2019). https://doi.org/10.1016/j.compositesb.2019.01.065
23. E. Ahmadloo, A.A. Gharehaghaji, M. Latifi, H. Saghafi, N. Mohammadi, Effect of PA66 nanofiber yarn on tensile fracture toughness of reinforced epoxy nanocomposite. Proc IMechE Part C: J Mech. Eng. Sci. (2018). https://doi.org/10.1177/0954406218781910
24. ASTM D 4762-18, *Standard Guide for Testing Polymer Matrix Composite Materials* (ASTM International, USA, 2008)
25. ASTM D 2344/D2344M-16, *Standard Test Method for Short-beam Strength of Polymer Matrix Composite Materials and their Laminates* (ASTM International, USA, 2016)
26. ASTM D 638-14, *Standard Test Method for Tensile Properties of Plastics* (ASTM International, USA, 2014)
27. E. Zussman, M. Burman, A.L. Yarin, R. Khalfin, Y. Cohen, Tensile deformation of electrospun nylon-6,6 nanofibers. J. Polym. Sci. Part B: Polym. Phys. **44**(10), 1482–1489 (2006). https://doi.org/10.1002/polb.20803
28. R. Palazzetti, Electrospun nanofibrous interleaves in composite laminate materials. PhD Thesis, University of Bologna (2014)
29. I. Alghoraibi, Fabrication and characterization of polyamide-66 nanofibers via electrospinning technique: effect of concentration and viscosity. Int. J. ChemTech Res. **7**(01), 20–27 (2015)
30. F. Kayaci, H.S. Sen, E. Durgun, T. Uyar, Electrospun nylon 6,6 nanofibers functionalized with cyclodextrins for removal of toluene vapor. J. Appl. Polym. Sci. (2015). https://doi.org/10.1002/app.41941
31. A. Anand, N. Kumar, R. Harshe, M. Joshi, Glass/epoxy structural composites with interleaved nylon 6/6 nanofibers. J. Compos. Mater. **51**(23), 3291–3298 (2016). https://doi.org/10.1177/0021998316682603
32. B. Beylergil, M. Tanoglu, E. Aktas, Enhancement of interlaminar fracture toughness of carbon fiber–epoxy composites using polyamide-6,6 electrospun nanofibers. J. Appl. Polym. Sci. (2017). https://doi.org/10.1002/app.45244
33. T.V. Kumar, M. Chandrasekaran, V. Santhanam, N. Udayakumar, Characterization of nylon 6 nano fiber/E-glass fiber reinforced epoxy composites. IOP Conf. Ser.: Mater. Sci. Eng. **183**, 012002 (2017). https://doi.org/10.1088/1757-899X/183/1/012002
34. M.K. Akkapeddi, Glass fiber reinforced polyamide-6 nanocomposites. Polym. Compos. **21**(4), 576–585 (2000). https://doi.org/10.1002/pc.10213
35. S.M. Kale, P.M. Kirange, T.V. Kale, N.J. Kanu, E. Gupta, S.S. Chavan, U.K. Vates, G.K. Singh, Synthesis of ultrathin ZnO, nylon-6,6 and carbon nanofibers using electrospinning method for novel applications. Mater. Today: Proc. (2021). https://doi.org/10.1016/j.matpr.2021.06.289
36. N.J. Kanu, A. Lal, Nonlinear static and dynamic performance of CNT reinforced and nanoclay modified laminated nanocomposite plate. AIP Adv. **12**, 025102 (2022). https://doi.org/10.1063/5.0074987
37. N.J. Kanu, Modeling of stress wave propagation in matrix cracked laminates. AIP Adv. **11**, 085217 (2021). https://doi.org/10.1063/5.0057749
38. A. Lal, N.J. Kanu, The nonlinear deflection response of CNT/nanoclay reinforced polymer hybrid composite plate under different loading conditions. IOP Conf. Ser.: Mater. Sci. Eng. **814**, 012033 (2020). https://doi.org/10.1088/1757-899X/814/1/012033
39. N.J. Kanu, E. Gupta, V. Sutar, G.K. Singh, U.K. Vates, An insight into biofunctional curcumin/gelatin nanofibers, in *Nanofibers. Nanofibers—Synthesis, Properties and Applications*, ed. by B. Kumar (IntechOpen, 2021). https://doi.org/10.5772/intechopen.97113